NATIONAL TRANSPORTATION SAFETY BOARD
Office of Aviation Safety
Washington, D.C. 20594

April 5, 2022

Airworthiness Sub-Group Chairman's Factual Report

DCA21FA085

A. ACCIDENT

Operator:	United Airlines
Location:	Broomfield, CO
Date:	February 20, 2021
Time:	1309 mountain standard time (MST)
Airplane:	Boeing 777-222, N772UA

B. AIRWORTHINESS SUB-GROUP

Chairman: Scott Warren
National Transportation Safety Board
Washington, D.C.

Member: Doug Mansell
Federal Aviation Administration
Seattle, WA

Member: Kevin Johnson
United Airlines
Chicago, IL

Member: Jim Alves
Parker Hannifin Corporation
Irvine, CA

Member: Mostafa Donyanavard
ITT Inc., Connect and Control Technologies
Valencia, CA

Member: Mitch Hunt
International Brotherhood of Teamsters
Denver, CO

Member: Joe Hardin
Boeing Commercial Airplanes
Seattle, WA

C. SUMMARY

On February 20, 2021, about 1309 mountain standard time (MST), United Airlines flight 328, a Boeing 777-222, N772UA, experienced a failure of the right engine, a Pratt & Whitney PW4077, while climbing through an altitude of about 12,500 feet mean sea level (msl) shortly after takeoff from Denver International Airport (DEN), Denver, Colorado. There were no injuries to the 239 passengers and crew onboard, and the airplane sustained minor damage. The regularly scheduled domestic passenger flight was operating under the provisions of Title 14 Code of Federal Regulations (CFR) Part 121 from DEN to Daniel K. Inouye International Airport (HNL), Honolulu, Hawaii.

A secondary focus of this investigation has been on the failure of an engine driven pump supply shutoff valve to close and shut off the flow of hydraulic fluid to the affected engine when a flight deck fire handle was operated. An airworthiness sub-group was established to investigate the operation and condition of this valve. The airworthiness sub-group convened (some members virtually and some members in person) on May 11, 2021 and May 20, 2021 at ITT Inc., Connect and Control Technologies (ITT), Valencia, CA and on July 22, 2021 at Boeing's Equipment Quality Analysis (EQA) labs in Seattle, WA.

D. DETAILS OF THE INVESTIGATION

1.0 May 11, 2021 – examination of engine driven pump (EDP) supply shutoff valve at ITT in Valencia, CA.

According to ITT, the motor operated valve was manufactured by ITT Aerospace Controls in April of 1999 and was distributed through Parker to Boeing.

The shipping box containing the valve was retrieved from secure storage, and there was no apparent damage. The valve was removed from the box, and an external examination was conducted with no obvious damage noted (see figure 1). The valve data plate was photographed. The valve pins were photographed – no bent pins or corrosion was noted.

Figure 1
EDP supply shutoff valve – overall view

The valve cover was removed, and within the valve housing, on the port B side, debris buildup with an embedded silver piece was noted. The silver piece came off easily with a screwdriver, and it was placed in a plastic bag. A cotton swab was used to gather paste build up material and placed in a plastic bag. Very small black particles were noted in the seal area (not the o-ring) polymer in both ports. The small black particles were removed with a cotton swab from the tan seal area and placed in a plastic bag.

There was powder/paste like debris noted on the output shaft around the manual arm on the actuator side of the mounting plate.

A tag reading "MR 29026-1" was noted, and according to group members, this was a tag applied by United when the part was originally received by them and was no longer used.

Note 32 of ICD AV16B2211 for this motor operated valve provided for the return of the part to ITT for an updated valve assembly (PN 125838CM-1) for improved open-to-close operation. If this update had been performed there should have been a marking on the side of the valve. No such marking was

found.

There were no other markings indicating the incorporation of any other service bulletins or other overhauls.

The data plate for the valve included the following information:

P/N – Boeing S271W741-22
S/N – T50052
P/N – Parker 2960034-101
3HA89 mfr 99-04

Continuity checks were performed between the pins of the connector. Negative and positive leads were switched to measure continuity in both orientations. The continuity checks all produced a result of "open circuit" except for the pin/lead combinations shown in table 1.

Table 1
Connector pin continuity results 1

Negative lead on pin:	Positive lead on pin:	Result
1	3	26.5 MOhms
1	7	25.6 MOhms
2	4	0.2 Ohms
3	7	0.2 Ohms
8	Chassis ground	0.1 Ohm

Positive lead on pin:	Negative lead on pin:	Result
1	3	285.6 kOhms
1	7	285.6 kOhms
2	4	0.1 Ohms
3	7	0.2 Ohms
8	Chassis ground	0.3 Ohm

The bonding and grounding test was conducted, and a value of 8.12 mOhm was noted for testing between Pin 8 and the mounting surfaces when using 1 amp current.

The running current test was attempted. The zip tie restraining the indicator arm was removed, and the valve was installed in the ITT hydraulic flow test bench (see figure 2). The voltage applied to the valve was 18 v, with 100 psig applied, and the valve did not close and there was no current draw noted on the test setup.

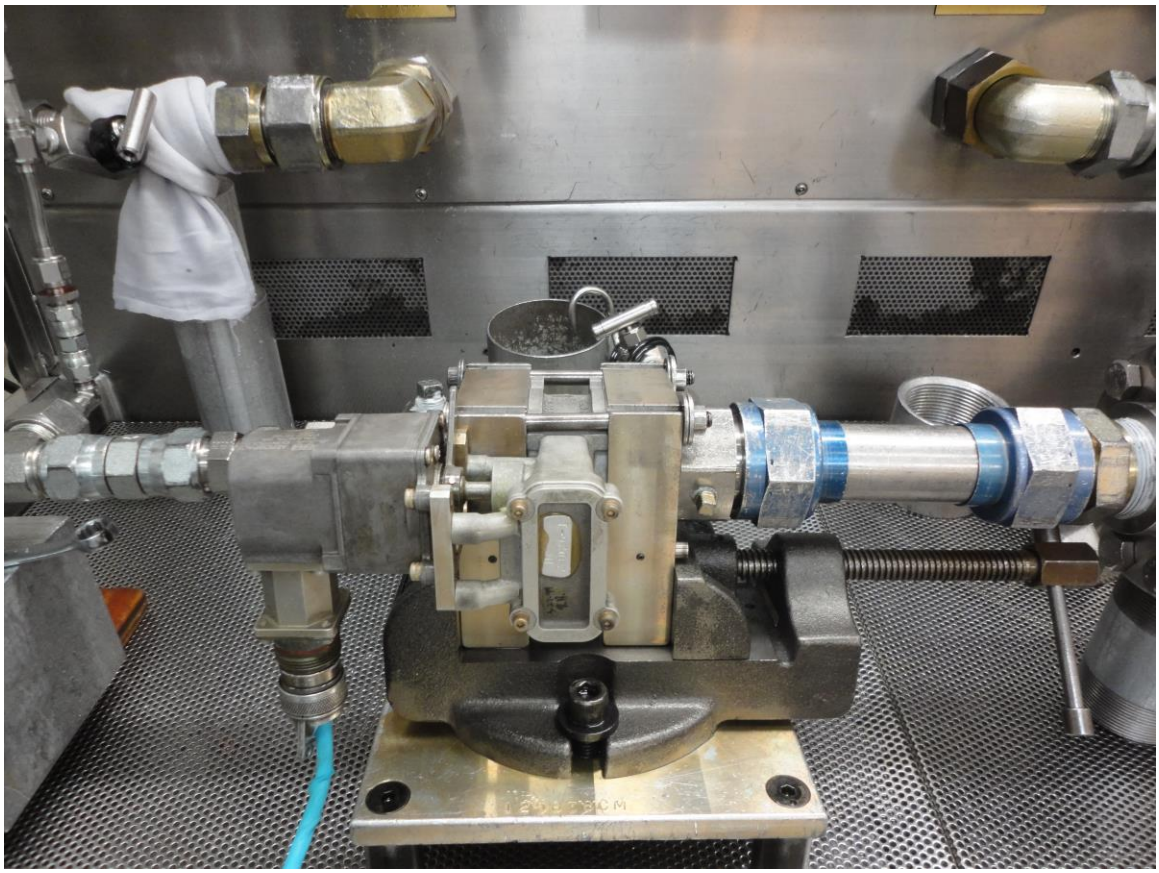

Figure 2
Valve installed on test bench

The continuity checks were repeated for the motor related connector pins with the results shown in table 2:

Table 2
Connector pin continuity results 2

Negative lead on pin:	Positive lead on pin:	Result
1	3	Open circuit
1	7	Open circuit

Positive lead on pin:	Negative lead on pin:	Result
1	3	269.6 kOhms
1	7	269.5 kOhms

The team decided to pull the actuator from the accident unit and install a known good actuator.

The accident actuator looked ok when removed. A voltage of 18 v was applied to the accident actuator after removal with no load applied, and the actuator did not

move. When the accident valve was mated with a known good actuator, the valve operated with a test setup of 18 volts, 50 gpm flow rate at 100 psig. The diode within the accident actuator was tested, and showed a good diode drop of 0.591 volts when tested.

The team decided to stop the examination at this point and determine the next steps. The valve components were all placed in a box and stored at ITT.

2.0 May 20, 2021 – Continuation of examination of engine driven pump (EDP) supply shutoff valve at ITT in Valencia, CA.

The shipping box containing the valve was retrieved from secure storage, and there was no apparent damage. An exemplar relay provided from ITT stock for CT scanning was removed from the box and taken by ITT personnel.

Continuity checks were repeated on the valve using the connector pins, and the results are shown in table 3.

Table 3
Connector pin continuity results 3

Negative lead on pin:	Positive lead on pin:	Result
1	3	Open circuit
1	7	Open circuit

The current draw through the motor was checked with 28 v applied, and 1 mA was measured and noise in the meter reading was noted.

The bolts were removed to allow for removal of the valve cover. No axial play was noted in the shaft when pulled. Some axial play was noted in the output indicator when pulled. Feeler gauges were used to measure clearance between the position indicator and the valve body, and a measurement of 0.001 inches was noted. This was an acceptable value according to ITT documents.

The position indicator arm was removed.

The screws holding the actuator cover to the body were removed, and the cover was removed. No debris, water, corrosion, or streaking was noted inside the actuator body or on the cover (see figure 3).

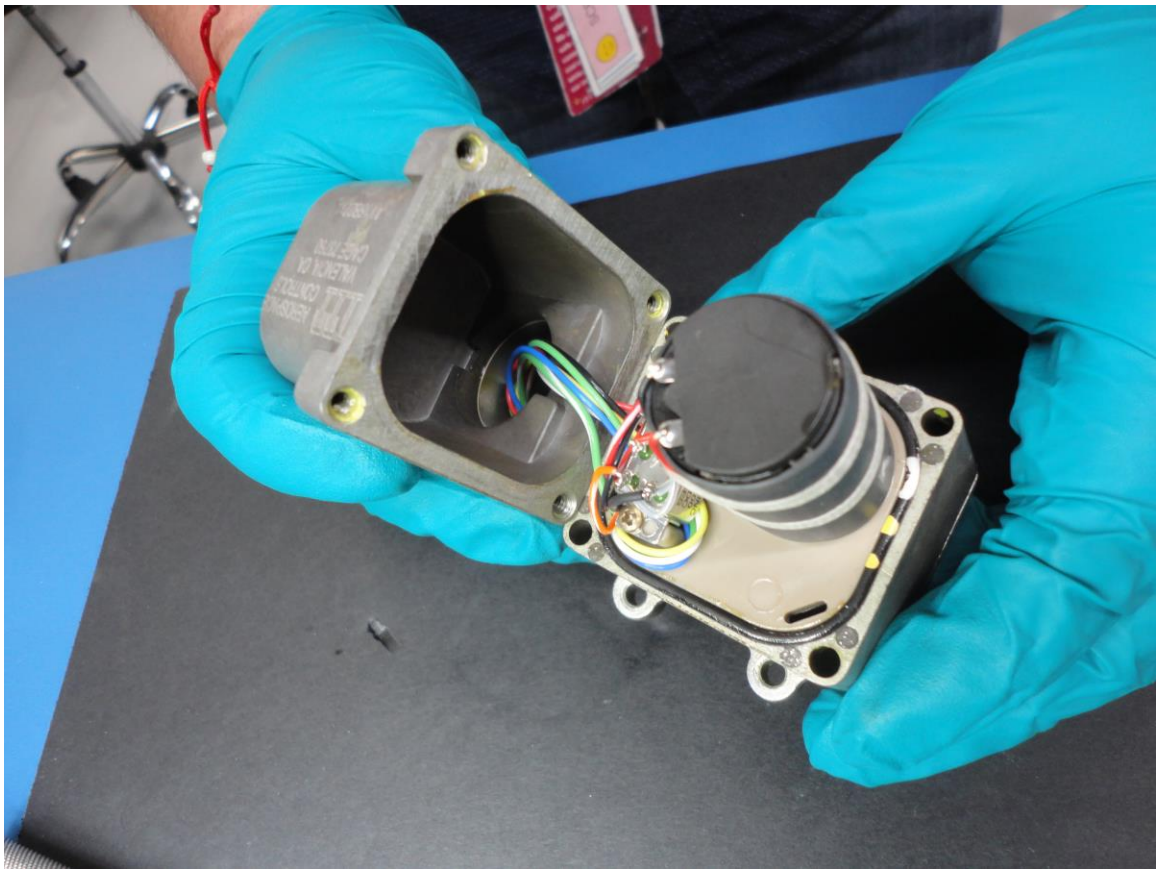

Figure 3
Actuator cover removed

Lacing tape on the motor was found to be white – not discolored. There was no burned smell within the actuator body. There were no indications of overheating within the actuator body noted. All of the solder joints looked ok, and the insulation within the body did not look discolored or overheated. The diode was inspected and was not discolored. The wires to the relay were all checked for proper placement and solder security – all were found to be ok.

A continuity check was conducted across the motor terminals. With the positive lead on the positive terminal and the negative lead on the negative terminal, the tester indicated an open circuit.

The resistance levels between the connector pins 1 and 3 and the relay pins was measured with the results shown in table 4.

Table 4
Connector to relay pin continuity results

Connector pin	Relay pin	Result
1	X1	0.4 Ohms
1	X2	0.3 Ohms
1	A1	0.3 Ohms
1	A3	0.3 Ohms
1	B1	0.3 Ohms
3	B3	0.3 Ohms
B2	Motor + terminal	0.4 Ohms
A2	Motor – terminal	0.5 Ohms
A2	A3	1.4 Ohms
B2	B3	1.4 Ohms
A1 (positive lead)	A2 (negative lead)	0.8 Ohms
A1 (negative lead)	A2 (positive lead)	0.1 Ohms
B1 (positive lead)	B2 (negative lead)	2.75 kOhms
B1 (negative lead)	B2 (positive lead)	Open circuit

The valve was manually moved to the closed position, and the switch circuit indications were measured using the connector pins. The movement of the valve was noted to be smooth and unremarkable. Continuity checks were repeated on the valve using the connector pins, and the results are shown in table 5.

Table 5
Connector pin continuity results 4

Positive pin	Negative pin	Result
2	1	704 Ohms
6	1	704 Ohms
6	2	0.2 Ohms
5	3	0.2 Ohms
Chassis	8	0.2 Ohms

The motor was removed and inspected with no obvious faults found. The lacing was cut and the wires to the motor terminals were cut. The gears on the output of the motor looked ok with no debris noted. White grease was noted as being present on the gears.

Note 33 of ICD AV16B2211 for this motor operated valve provides for the return of the part to ITT to change the valve gear lubrication from lubriplate grease (which is white) to Aeroshell 33 grease (which is not white). If this update had been performed the letter “A” should have been inserted after the serial number. No such marking was found.

The brush-to-brush continuity was noted to be between 200 Ohms and 700 Ohms. The value changed during disassembly. According to ITT personnel, the motor has carbon/copper brushes with copper commutator bars.

Resistance measurements were taken across the motor terminals as the commutator bars were rotated. The initial position of the commutator bars was noted by placing a black mark on the bar visible through a window in the bottom of the motor – this bar was denoted as "bar 1". The bars were then listed as 1 through 9, with the rotation of the motor being counterclockwise when viewed from the shaft/pinon side. The resistance values across the motor terminals were as noted in table 6.

Table 6
Resistance values across the motor terminals with the noted commutator bar visible in the motor window

Commutator bar	Result
1	300 Ohms
2	108 Ohms
3	1067 Ohms
4	40 kOhms
5	240 kOhms
6	285 Ohms
7	97 Ohms
8	3.2 kOhms
9	138 Ohms

The examination was stopped at this point, and the valve components were placed in the box for storage at ITT.

3.0 July 22, 2021 – Continuation of examination of engine driven pump (EDP) supply shutoff valve at Boeing EQA labs in Seattle, WA.

The full results of Boeing's examinations are contained in attachment A. Highlights of the examinations conducted with the group present are shown below.

ITT hand carried the shipping box containing the valve to the EQA labs, and it was examined with no apparent damage noted. The entire valve was transported to the EQA labs, but only the motor was removed from the box.

An index mark was applied to the pinion tooth and ring surrounding to show the initial position of the motor shaft. The pinion teeth were examined under an optical microscope, and all of the teeth looked ok. The sleeving around the

motor was removed. There were no signs of moisture on the inside of the sleeve or on the motor exterior.

Nomenclature on the motor exterior was:
P/N: 125735AJ – identified as the ITT motor P/N with the pinion installed
P/N: 23LT2R 12 216E 119
125734V – motor P/N without pinion

Escap ZS

Swiss made
10 98 (manufactured in October 1998)
554T (configuration control)

The rear cover of the motor was removed with a flat blade. The brush wires were exposed and examined. The brush cap was removed using a soldering iron to melt the plastic tabs.

There was a black strip of material on the collector bars that corresponded to the running surface for the brushes. The motor was checked for bridging of one collector bar to another and none was found. Both brush contact surfaces were examined, and they looked similar to each other.

The pinion gear was removed by grinding the weld off and allowing the pinion gear to be removed from the end of the motor shaft. Pliers were used to hold the pinion gear in place during grinding. The motor was covered with tape to prevent material from going into the motor.

The E-clip, 2 washers, spring washer, and a spacer were removed. The motor bearing on the E-clip end was examined with no defects noted. The rotor was pushed through the housing and removed from the motor. The upper bearing was examined with no defects noted.

A runout test was conducted on the commutator bars. The results are shown in attachment A.

The brushes and commutator bars were released to Boeing for additional examination with the understanding the Boeing would cut one or more of the commutator bars to allow for detailed examinations. The results of the additional work are contained in attachment A.

Scott Warren
Lead Aerospace Engineer

Attachment A

Boeing Equipment Quality Analysis (EQA) Report
Boeing Analytical Chemistry Lab Report
Boeing Engineering Test and Technology Report

Equipment Quality Analysis Report

Boeing Commercial Airplanes

TO: Air Safety Investigations (ASI)

EQA NUMBER: AS13384

DATE: December 13, 2021

MODEL NUMBER: 777-200

AIRPLANE NUMBER: WA005

SUBJECT: ***Motor Operated Gate Valve In-Flight Incident: Direct Current (DC) Motor Examination***

IDENTIFICATION:

Part name:	Motor Operated Gate Valve
Boeing part number:	S271W741-22
Supplier part number:	2960034-101 (Parker Hannifin Corporation)
Supplier part number:	AV16B2211 (ITT Aerospace Controls)
Serial number:	T50052
Supplier:	Parker Hannifin Corporation and ITT Aerospace Controls
Manufactured date:	99-04

REFERENCES:

(a) National Transportation Safety Board (NTSB) I.D. DCA21FA085.
(b) ITT Aerospace Controls CMM: 29-10-15 (Motor Operated Gate Valve)
(c) ITT Aerospace Controls CMM: 29-11-15 (DC Motor Operated Actuator Assembly)

BACKGROUND:

As reported in the reference (a) NTSB case number, on Feb 20, 2021, a United Airlines (UAL) 777-200, variable number WA005, experienced a fan blade out (FBO) engine failure of the right engine while on climb out from Denver International Airport (DEN).

Airplane WA005 was delivered on September 29, 1995, and was reported to have accumulated approximately 96,975 hours and 17,784 cycles at the time of the engine failure.

Additional information, provided by ASI, reported that after the event, a Motor Operated Valve (MOV), installed as an Engine Driven Pump (EDP) shutoff valve in the Right Hydraulic System, was found in the “open” position. The MOV should have been in the “closed” position after the flight deck fire handle was operated during the event. The fire handle was later verified to be still in the extended position, indicating the MOV did not operate during the event. It was also verified that power to the MOV pin was present indicating the cause of failure was due to the valve non-operation.

The supplier (ITT Aerospace Controls) performed a teardown examination of the subject MOV on May 11 and 20, 2021 and confirmed the non-operating condition. Troubleshooting was performed and isolated to a high resistance condition at the Direct Current (DC) motor of the MOV actuator assembly.

Under direction of the US National Transportation Safety Board (NTSB), Boeing Air Safety Investigation (ASI) requested Boeing Equipment Quality Analysis (EQA) examination of the subject DC motor.

SUMMARY:

Boeing EQA performed the complete examination of the subject DC motor. Under direction of the NTSB, the subject DC motor was disassembled. The part markings, terminals, commutators, brushes, torsion springs, bearings and pinion gear were photo-documented. Runout measurements were performed on the commutators. Electrical resistance measurements were performed between commutators. Chemical analyses were performed on the black material present on the commutators and brush working surfaces. All images and analyses were provided to Boeing ASI.

EXAMINATION:

Figure 1 shows an overview image of the MOV assembly, the actuator assembly and the DC motor location. Images were taken from references (b) and (c) of the CMMs.

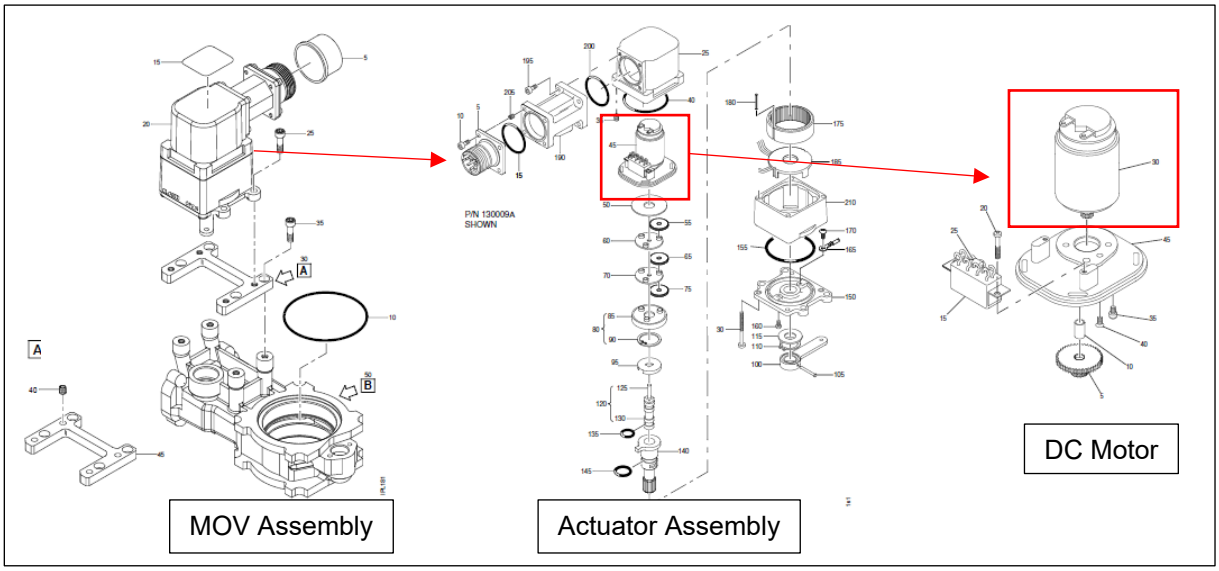

Figure 1: MOV assembly, Actuator assembly and DC Motor location shown.

Examination of the DC motor was conducted on July 22, 2021 at the Boeing EQA facility, with Boeing ASI, Boeing Design Engineering (DE), ITT representatives, Portescap representative and UAL representative in attendance. Remote attendees included the NTSB and Portescap supplier.

The MOV assembly was hand carried to the Boeing EQA facility by the ITT representatives and received as shown on Figure 2.

Figure 2: Box containing the MOV assembly.

The box was opened and a bag containing the DC motor was identified as shown on Figure 3.

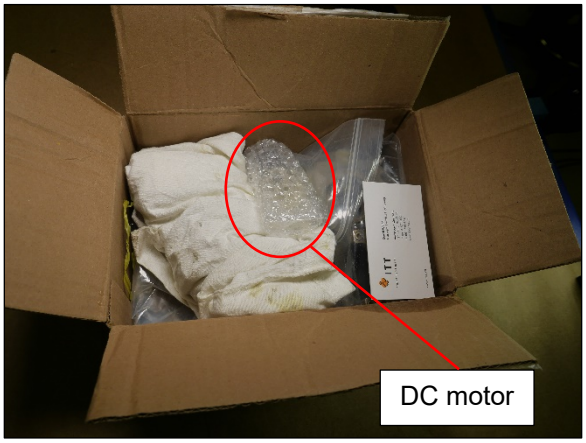

Figure 3: Box opened and bag containing DC motor identified.

The bag containing the DC motor was removed from the box. The rest of the parts remained inside the box. The DC motor was removed from the bag and a visual inspection was performed on its overall condition. A yellow post-it note was included in the bag. The black sleeve covering the DC motor housing was intact. Portions of the black and red wires were still present on the terminals. The back cover and pinion gear appeared unremarkable. Figure 4 shows an image of the DC motor removed from the bag. Back cover and pinion gear photographed for condition.

Figure 4: DC motor removed from bag. Pinion gear and back cover also shown.

Black ink was marked on one tooth of the pinion gear and adjacent section of housing for alignment as shown on Figure 5.

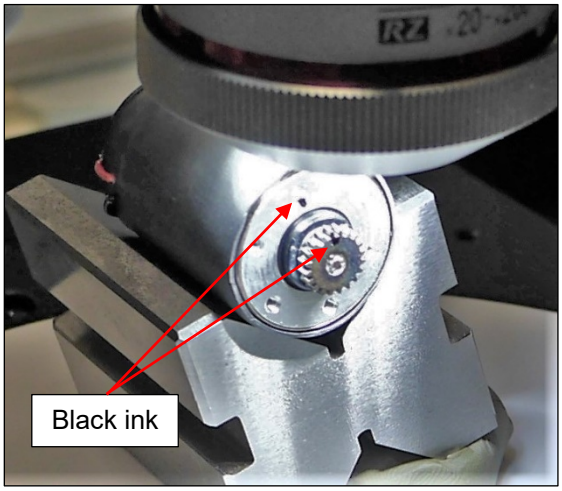

Figure 5: Black ink marked on tooth and housing for alignment.

The pinion gear was examined under magnification as shown on Figure 6. Fibrous-like material were observed at random locations and a translucent gel-like substance were present near the edges of the teeth. No deformations were observed on each tooth profile and base. The weld between the shaft and pinion gear appeared consistent and no anomalies observed.

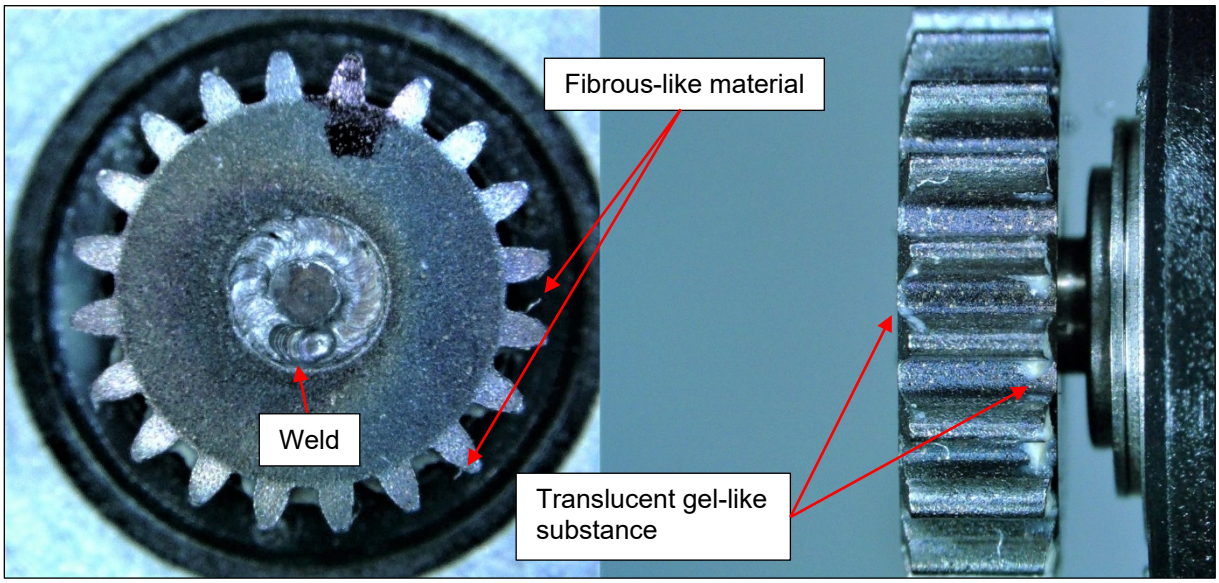

Figure 6: Pinion gear under magnification. Locations of weld, fibrous-like material and translucent gel-like material shown.

A sharp blade was used to cut the black sleeve open as shown on Figure 7. No visible sign of moisture or any contamination was present on the inner surface of the black sleeve and on the DC motor housing.

Figure 7: Black sleeve removed from the DC motor housing.

Part markings on the DC motor housing were photo documented as shown on Figure 8.

Figure 8: DC motor part markings.

The black plastic cap was removed as shown on Figure 9. A brown colored substance was visible on the black terminal. Solder appeared sufficient and no voids or cracks present. Tool marks were present on the black plastic material. ITT Aerospace Controls had previously removed the plastic cap on an earlier examination. Solder on both terminal wires and brush wires appeared unremarkable.

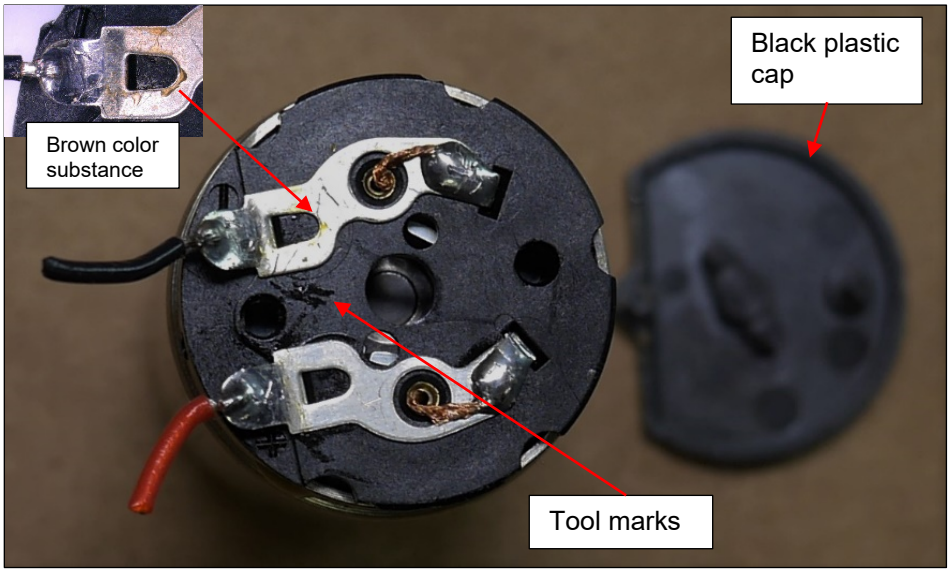

Figure 9: Black plastic cover removed from the rear section of the DC motor.

The wire strands on the brushes appeared kinked but no visible strands broken. Figure 10 shows a magnified image of the positive brush wire and Figure 11 shows a magnified image of the negative brush wire.

Figure 10: Positive brush wire.

Figure 11: Negative brush wire.

To access the commutators and brushes, the black round plastic tabs around the DC motor housing were melted using a soldering iron under direction of the NTSB. The use of soldering iron was discussed as a better alternative to using a small drill bit. A blade was wedged to separate the black plastic cover from the housing. Figure 12 shows the location of the plastic tabs and knife wedge location.

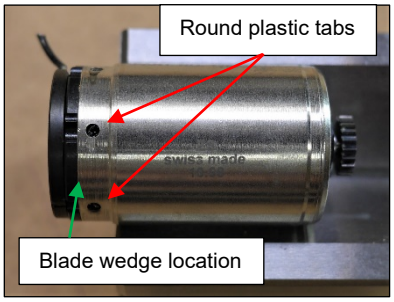

Figure 12: Location of plastic tabs and knife wedge placement.

Figure 13 shows the orientation of the brushes after separation from housing. Wire brushes appeared kinked but no visible strands broken.

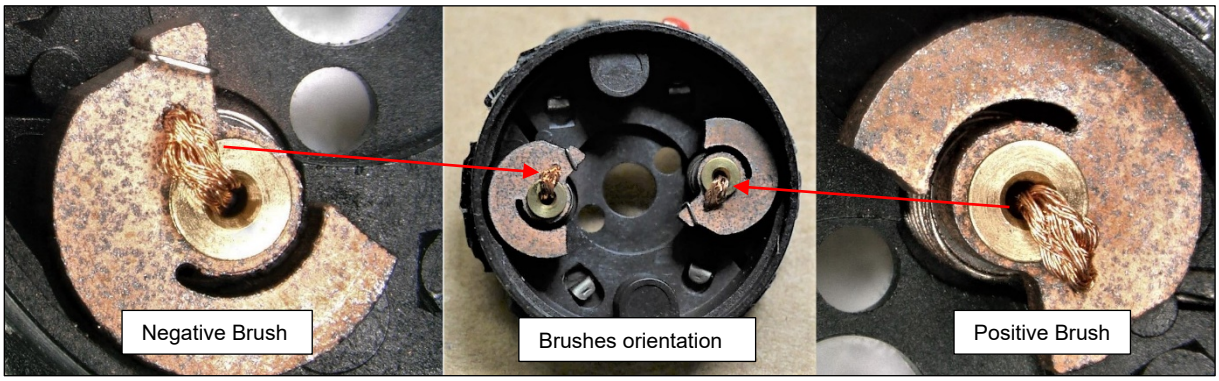

Figure 13: Orientation of brushes upon separation from DC motor housing. Magnified images of each brush showing wire strands.

The windings on each torsion spring were visually counted and yielded eight (8) turns on each brush as shown on Figure 14.

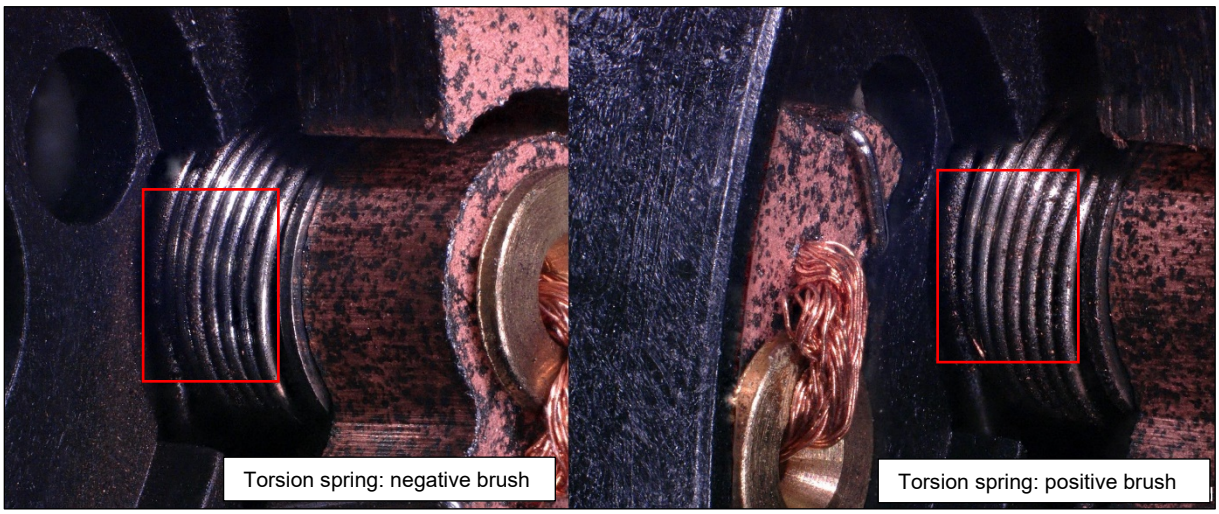

Figure 14: Negative and positive torsion springs.

Both brushes were examined under magnification as shown on Figure 15 and 16. Both brushes exhibited deep lines consistent with the commutator surfaces. Side view of both brushes appeared to take the shape of the commutators. A silver colored particle was present at the edge of the negative brush.

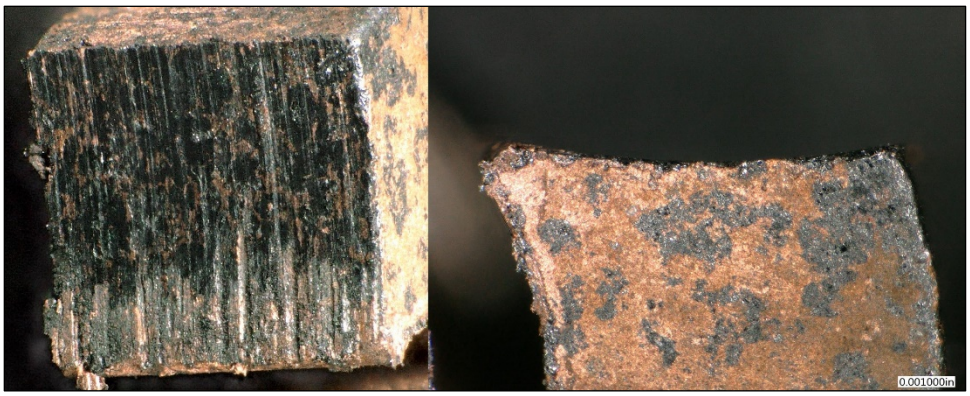

Figure 15: Positive brush top surface (left) and side view (right).

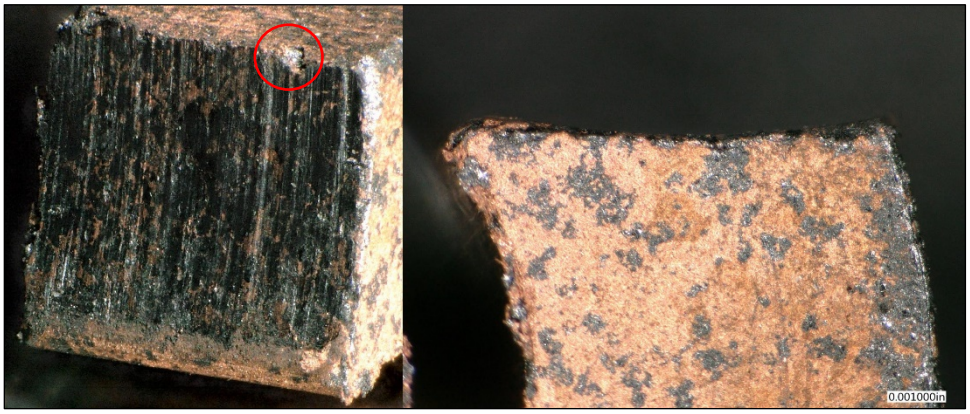

Figure 16: Negative brush top surface (left) and side view (right). Note: Silver colored particle observed circled in red.

One of the commutators contained a black mark at the top surface as shown on Figure 17. Supplier (ITT Aerospace Controls) previously marked the commutator as reference for obtaining resistance values. The commutators were labeled 1 thru 9 for reference.

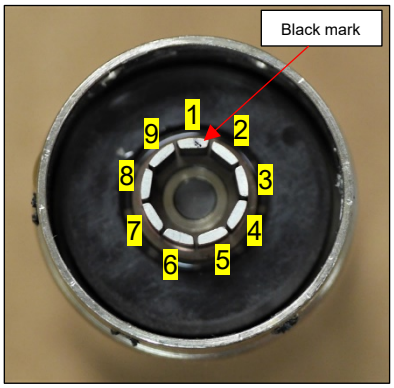

Figure 17: Commutators shown as viewed from the top. One commutator previously marked in black as reference.

Each commutator surface was examined under magnification as shown on Figure 18 thru 26. Varying amounts of black material were present and confined to the commutator surfaces that are in contact with the brushes.

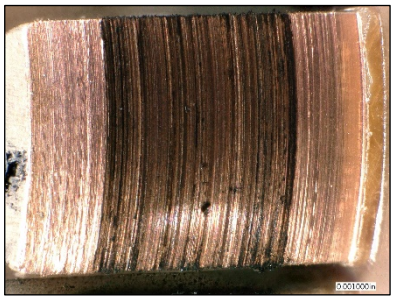

Figure 18: Commutator 1.

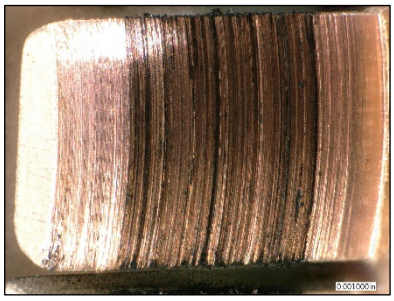

Figure 19: Commutator 2.

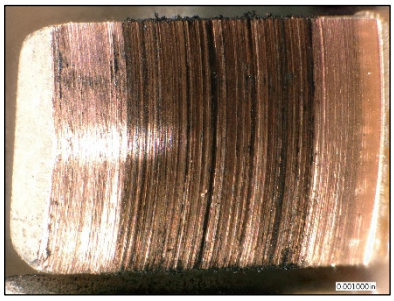

Figure 20: Commutator 3.

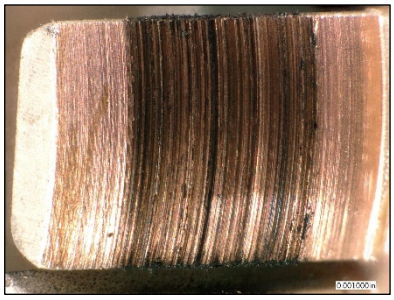

Figure 21: Commutator 4.

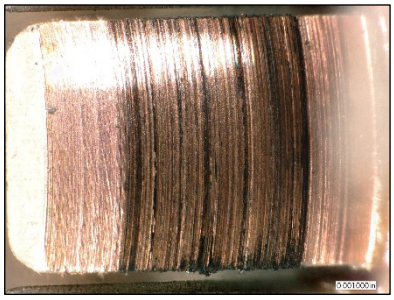

Figure 22: Commutator 5.

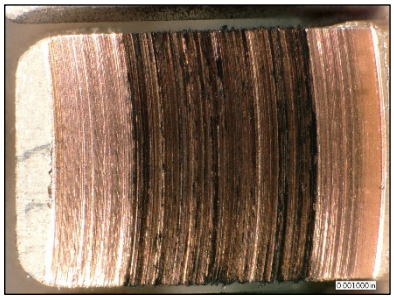

Figure 23: Commutator 6.

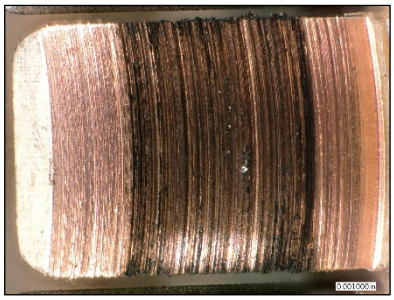

Figure 24: Commutator 7.

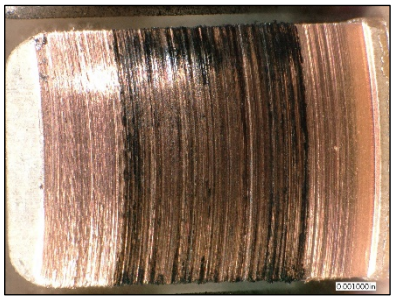

Figure 25: Commutator 8.

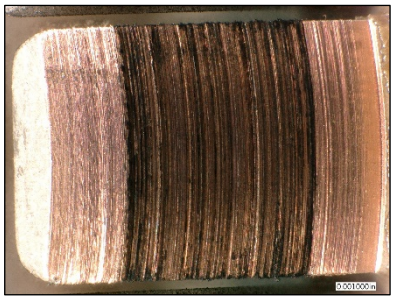

Figure 26: Commutator 9.

Black material buildup was present on the edges of the commutators but no bridging observed on adjacent commutators. Figure 27 show a representative image of the black material build up on the commutator edge.

Figure 27: Edge of commutator 5 with the black material buildup shown.

On commutator 7, silver colored particles were observed near the center as shown on Figure 28.

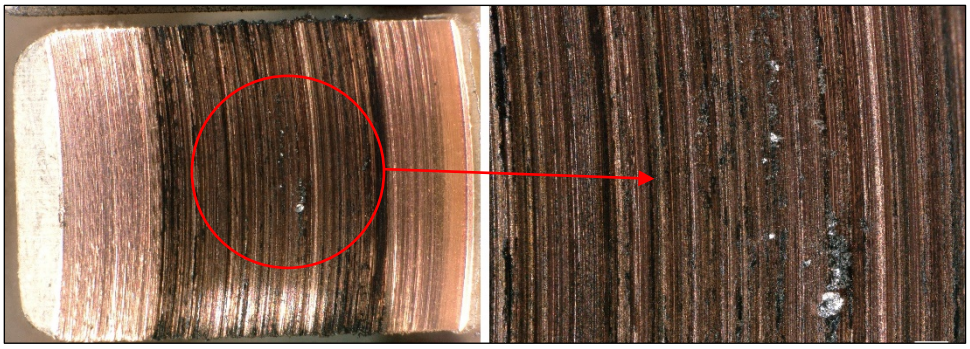

Figure 28: Silver colored particles present on Commutator 7.

The backside of the motor was covered with blue tape (Figure 29) to protect the commutators during removal of the pinion gear. The blue tape was not in contact with the commutator surfaces. A grinding tool was used under direction of the NTSB to separate the pinion gear from the shaft (Figure 30) to allow removal of the commutators from the housing.

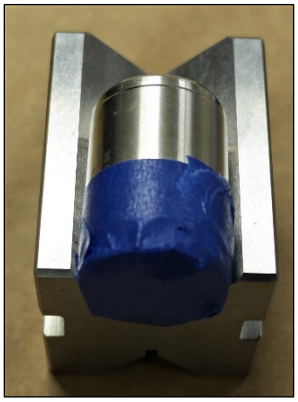

Figure 29: Backside of motor protected with blue tape.

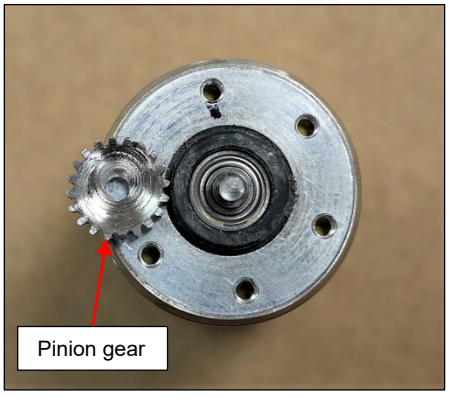

Figure 30: Pinion gear separated from the motor.

A spacer, spring disc, e-style retaining ring and two washers were located between the shaft and the pinion gear as shown on Figure 31.

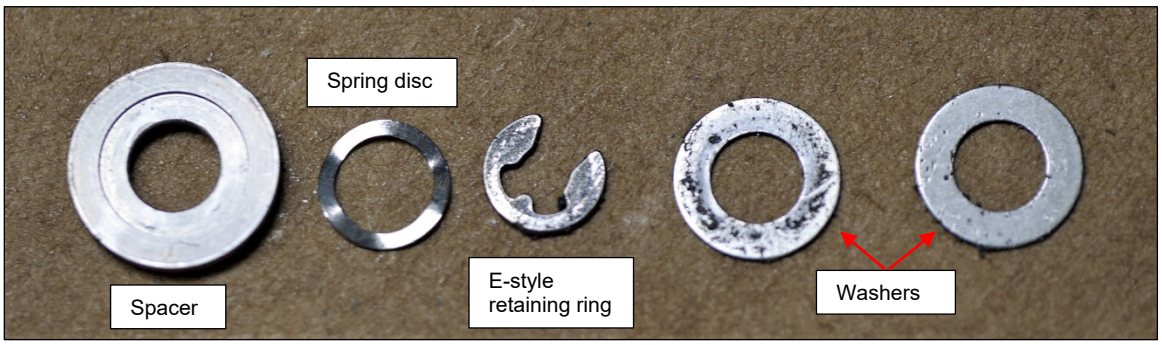

Figure 31: Component located between pinion gear and shaft.

The shaft was pushed out to separate the coil and commutators from the housing (Figure 32). The inner diameter of the coil was inspected under magnification and observed a silver colored particle (Figure 33) measuring 0.006769 inches.

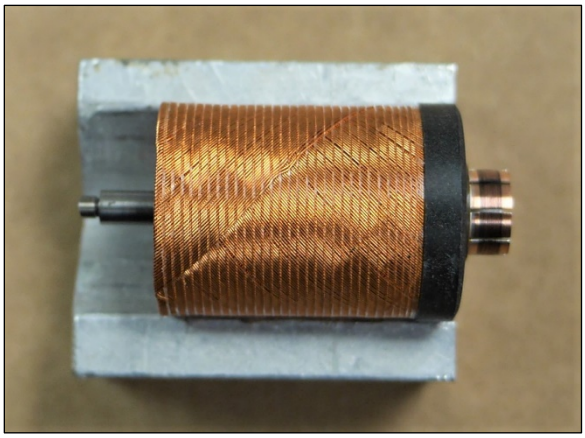

Figure 32: Coil with commtuators and shaft attached.

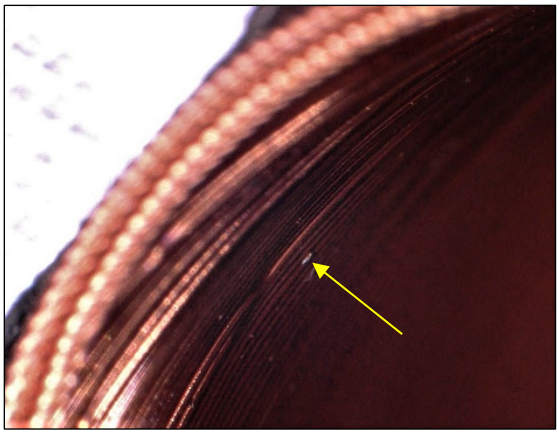

Figure 33: Inner diameter of coil showing location of silver colored particle.

Roundness profile was obtained on the commutator surfaces as shown on Figure 34. The top and bottom section of the commutators were subjected to roundness testing while the black band materials were avoided for preservation. The purpose of the roundness test was to determine the maximum amount of deviation between commutators.

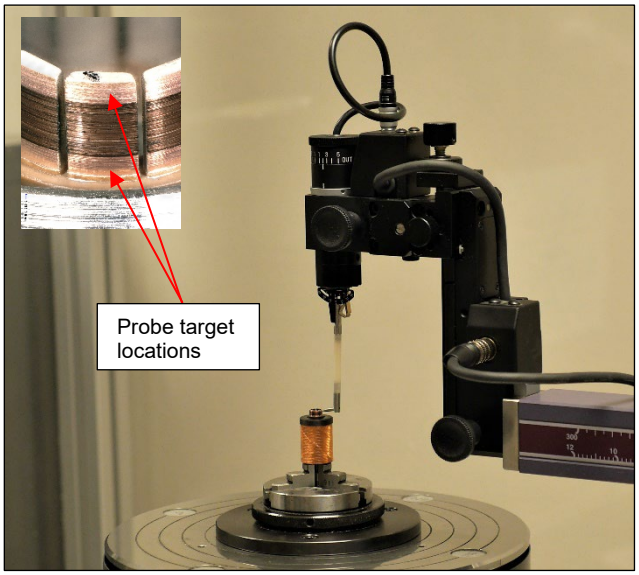

Figure 34: Commutators runout dimensioning.

Figure 35 shows a graph of the commutator roundness. Red lines represent the bottom section of the commutators while blue lines represent the top section of the commutators. The numbers represent the location of each commutator. Excluding the gaps between commutators, the lowest and highest point for the top and bottom sections were obtained.

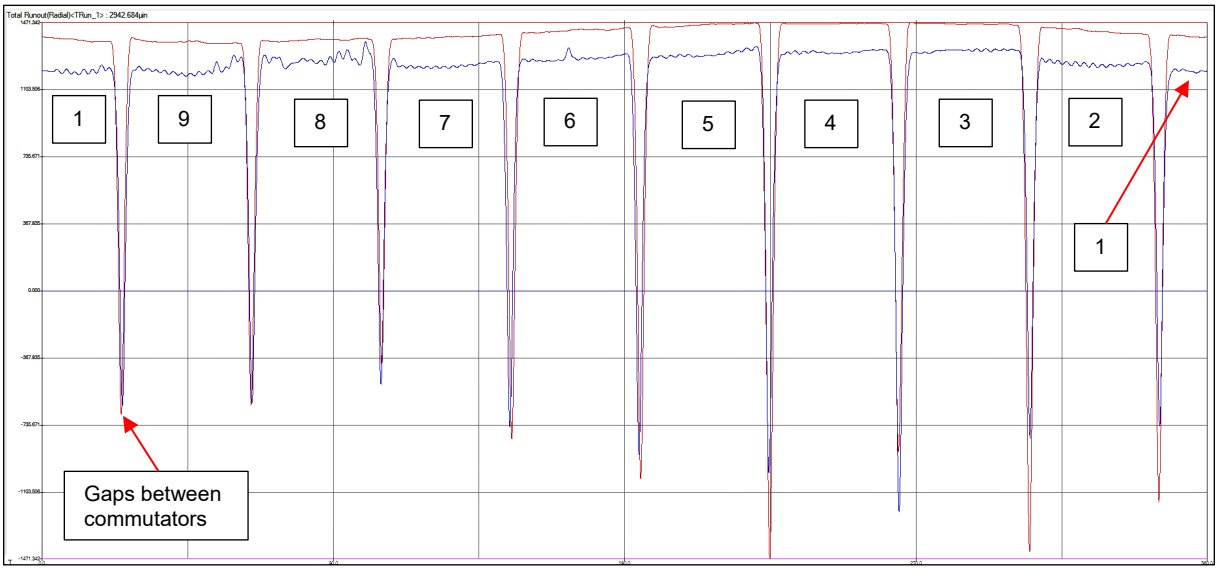

Figure 35: Roundness profile of the commutators.

Table 1 shows the measured highest and lowest point (excluding the gaps between commutators) for the top and bottom sections of the commutators. The deviation was calculated based on the difference between the highest point and lowest point for each section.

Table 1: Measured highest and lowest point for the top and bottom section of the commutators. Measurement are in micro-inches (μ-in). Commutator locations are also shown.

Graph Line	Highest Point	Commutator Location	Lowest Point	Commutator Location	Deviation (highest-lowest point)
Bottom Section Commutators (Red line)	1471.342	3,4,5	1357.075	9	114.267
Top Section Commutators (Blue line)	1371.358	8	1174.835	9	196.523

The resistance between commutators were measured. The commutators were probed at the top section to prevent damage on the surfaces where the black materials resided. Figure 36 shows the commutator numbering and location of probe for resistance measurements.

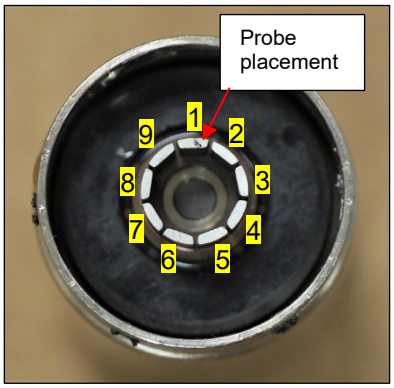

Figure 36: Commutator numbering and probe placement as shown.

Table 2 shows the recorded resistance measurements between commutators. Overall, the resistances appeared uniform: low resistance values between adjacent commutators and increased resistance values as the distance between commutators increased.

Table 2: Resistance measurements between commutators. Values are in ohms (Ω).

Commutator	1	2	3	4	5	6	7	8	9
1		2.7	4.6	6.0	6.7	6.6	6.0	4.6	2.7
2			2.6	4.6	5.9	6.5	6.5	5.9	4.6
3				2.7	4.7	5.9	6.6	6.6	6.0
4					2.8	4.9	6.0	6.8	6.8
5						2.9	4.8	5.9	6.6
6							2.9	4.7	6.0
7								2.9	4.8
8									2.8
9									

The front and rear bearings were inspected under magnification as shown on Figure 37. The front bearing appeared to show an opening between the inner race and the shield. The shield at the rear bearing appeared flushed at the inner and outer races.

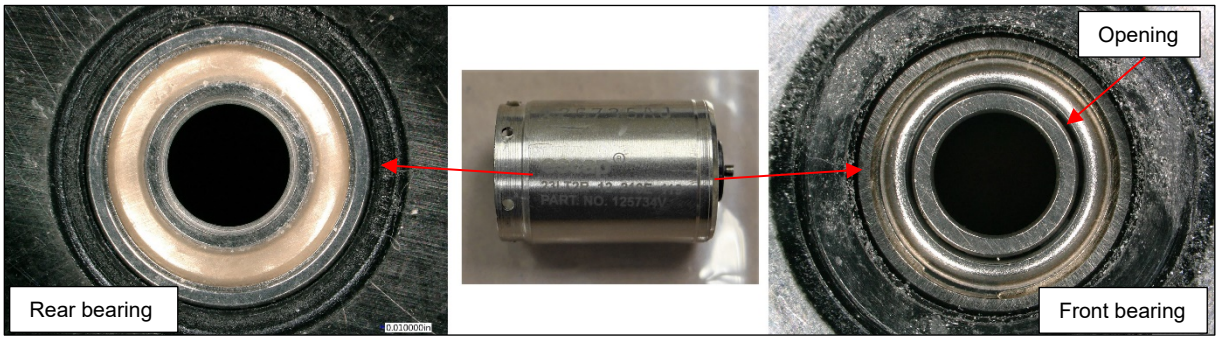

Figure 37: Rear and front bearings shown.

Prior to Boeing EQA performing the examination of the DC motor, ITT supplier performed the terminal resistance measurement for each commutator. Figure 38 shows the ITT supplier commutator numbering and Figure 39 shows the equivalent Boeing EQA commutator numbering. Table 3 shows the recorded resistance values for each commutator.

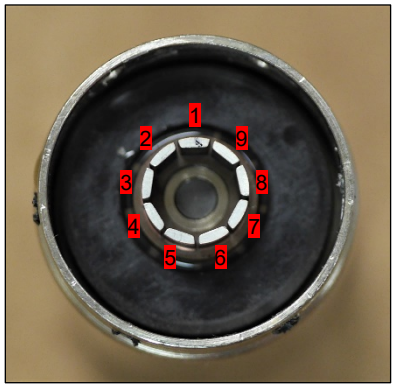

Figure 38: ITT supplier commutator numbering.

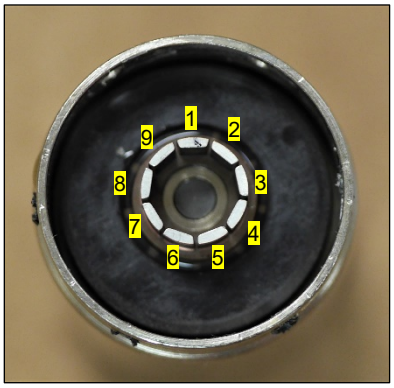

Figure 39: Boeing EQA commutator numbering.

Table 3: Terminal resistance values for each commutator provided by ITT supplier through Boeing ASI.

Commutator Number (ITT Supplier Numbering)	Terminal Resistance (Ohms)	Equivalent Commutator Number (Boeing EQA Numbering)
1	300	1
2	108	9
3	1.06K	8
4	40K	7
5	240K	6
6	285	5
7	97	4
8	3.2K	3
9	138	2

The two commutators with the highest resistance were identified as commutator 6 and 7 based on the Boeing EQA numbering system. The two commutators were separated from the rest of the commutators for black material identification analysis under direction of the NTSB. Figure 40 shows the steps taken in removing the subject commutators.

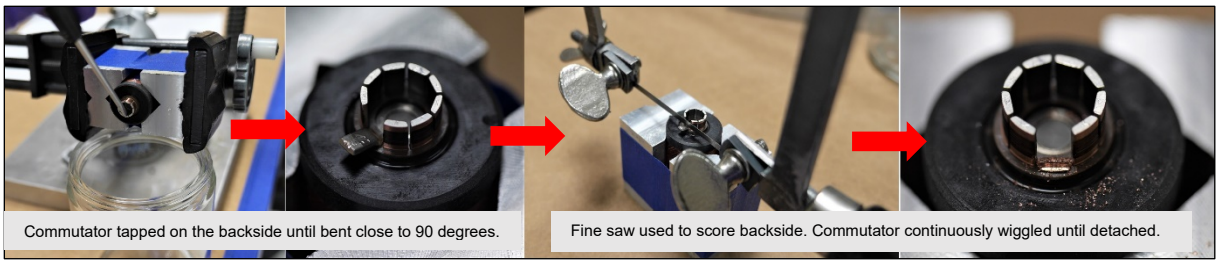

Figure 40: Steps in removing commutators as shown.

Conditions of commutator 6 and 7 removal were photo documented as shown on Figures 41 thru 44.

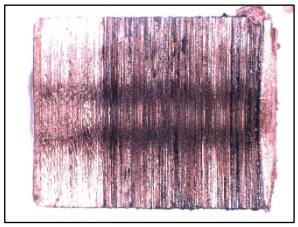

Figure 41: Commutator 6 surface in contact with brushes.

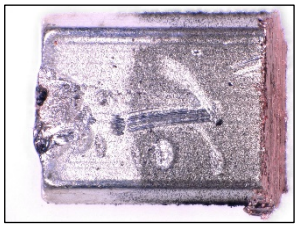

Figure 42: Commutator 6 backside.

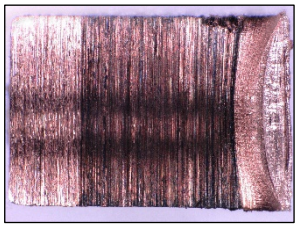

Figure 43: Commutator 7 surface in contact with brushes.

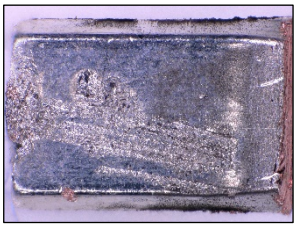

Figure 44: Commutator 7 backside.

To facilitate with the chemical analysis, the working surfaces (tip) of both brushes were isolated from the brush body. Figure 45 shows the steps in removing the brush.

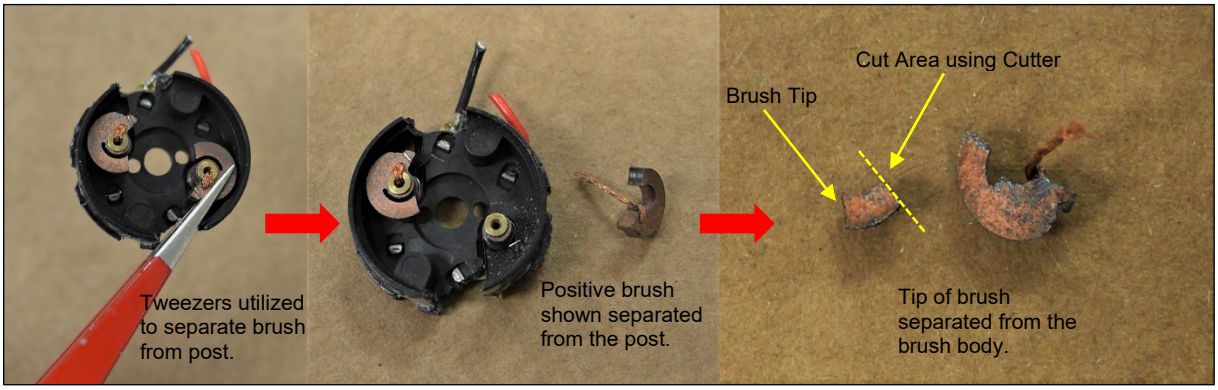

Figure 45: Steps in removing brushes shown.

After separation, conditions of the positive and negative brush were photo documented as shown in Figure 46.

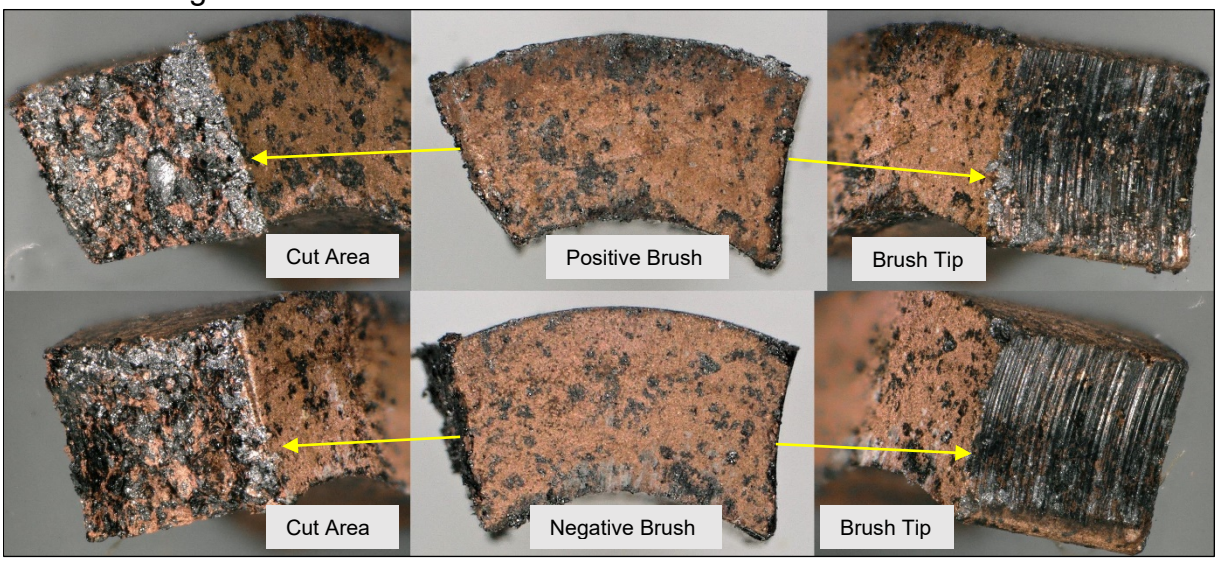

Figure 46: Positive and negative brush cut section.

ANALYSIS:

Boeing Research and Technology (BR&T) conducted a chemical analysis on black material present on commutators 6 and 7. Both working brush surfaces were also analyzed. The following is a summary of findings:

- Utilizing Fourier Transform Infrared Spectroscopy (FTIR), silicone was the only organic material identified on the working surfaces of commutators 6 and 7
- Utilizing FTIR, silicone was the most prevalent organic material identified on the working surfaces of both the positive (P) and negative (N) brushes
- Utilizing metallography, Scanning Electron Microscopy (SEM) and Scanning Transmission Electron Microscopy (STEM), silicone based substance was present on the working surfaces of the brush and commutator.
    - Silicone was found to be fully dense with copper metal and copper oxide fretting debris
    - The fretting debris was generated exclusively from the brushes

Enclosures A, B and C show the complete analysis reports from BR&T.

DISPOSITION:

The subject component will be conveyed per instruction from the NTSB and ASI after completion of this analysis.

The preceding information is being submitted for information purposes.

Signature on file.

ENCLOSURES:

A. FTIR on Commutators
B. FTIR on Brushes
C. Boeing AS13384 Motor Analysis - SEM/STEM of Commutators and Brushes

BOEING RESEARCH & TECHNOLOGY
Manufacturing and Manufacturing Technology
Chemical Technologies - Analytical Laboratories

Date: October 1, 2021

Analytical Chemistry Lab

[redacted]

DISTRIBUTION

To: [redacted]
Cc: [redacted]

Subject: AS13384 Material analysis, organic materials on commutators 6 & 7 from DC motor

Summary
Silicone was the only organic material identified on the surfaces of commutators 6 and 7.

Background
Commutators from DC motors were submitted for analysis in support of Air Safety investigation 13384. The commutators were removed from the DC motors by Equipment Quality Analysis (EQA) and placed into individual clean glass vials (with Teflon lined lids).

Figure 1 shows the sample #7, its container, and the tools used for analysis. All commutator samples were small pieces of metal with copper on the exterior surface of interest, rectangular in shape, approximately 0.15” tall x 0.10” wide.

On all commutators a black colored residue was formed on the surface of interest. The residue is expected from normal use. It was requested to determine what organic material was present on the surface of the commutators (both in the areas with black residue and without). SEM / EDS analysis will be performed subsequently on the commutators.

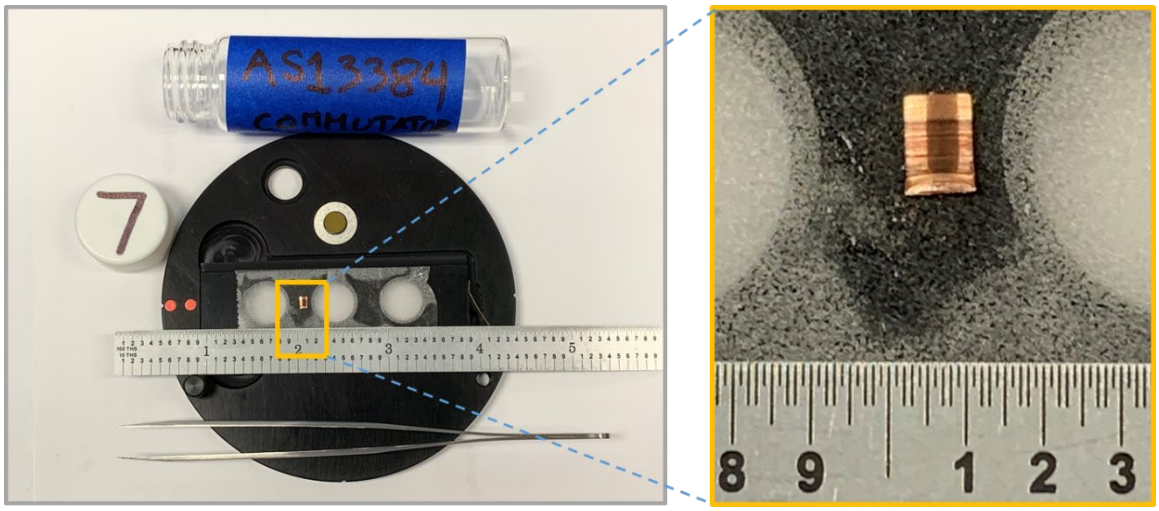

Figure 1. Pieces were transported in vials, handled with tweezers, and held on the sampling platform using double-stick tape.

[redacted]

Experimental

Samples were not cleaned or prepped beyond removing them from the vial with cleaned tweezers, and affixing them to a staging slide using double-stick tape. The sampling stage was mounted into a Thermo-Nicolet iN-10 FTIR microscope for scanning. The iN-10 was configured to generate "line maps" by collect a spectrum every 100 microns along a path set by the user, shown in Figure 2. Tick marks show where each spectrum was collected. Mapping went from bottom to top in Fig 2, starting at tick mark #1, which corresponded to "Spectrum #1". Each sample was scanned bottom to top along the center line and along the right side.

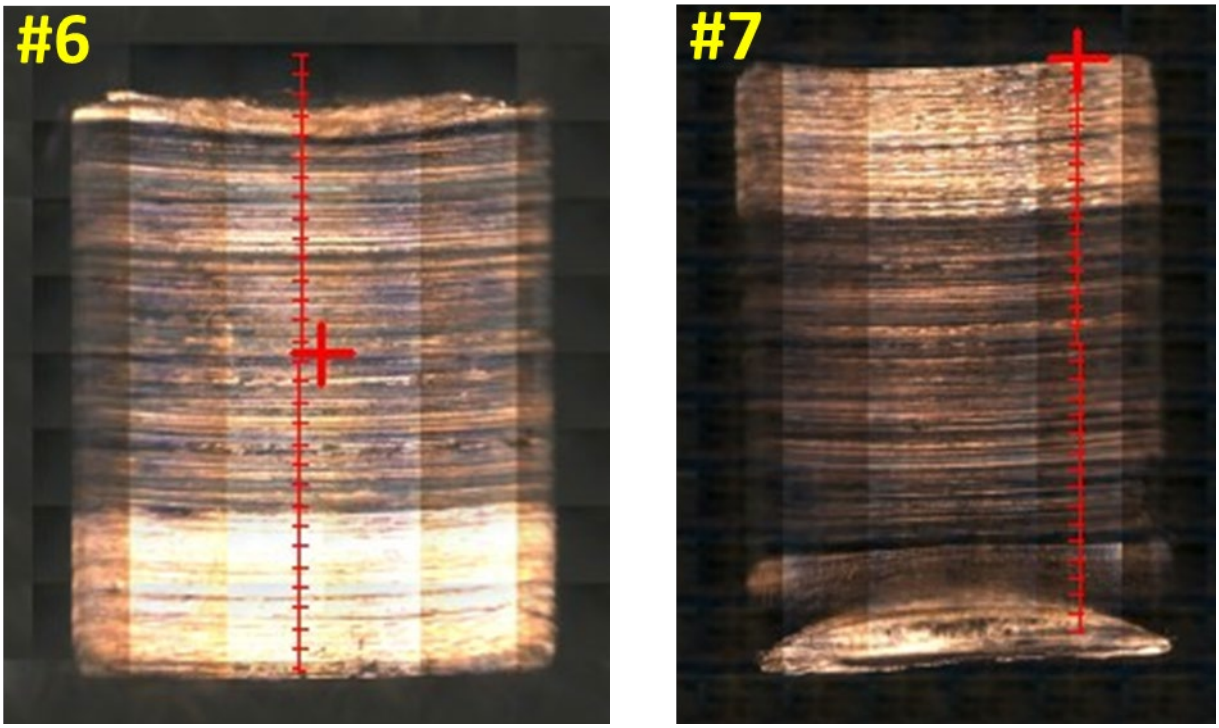

Figure 2. Screen shots from the iN-10. Red lines superimposed over samples show where data were collected. A spectrum was collected at each tick mark (every 100 microns).

Each spectrum was collected in reflectance mode, 132 scans co-averaged at 4 cm^{-1} resolution, over the range 750-4000 cm^{-1}, using a liquid nitrogen cooled MCT detector. The aperture was 100 microns x 100 microns. All spectra were screened to look for anomalies and trends. Standouts were analyzed in closer detail.

Results

Most of the surfaces of sample #6 and #7 were free of organic material. FTIR data from those areas contained only broad inorganic peaks, like the wide feature in Figure 3's red spectrum, from 1300-2500cm^{-1}, or purple spectrum from 1100-1700cm^{-1}.

Each commutator had traces of silicone. In sample #6, silicone was detected in the dark black stripe at the very top of the photo (tick marks 28-29). Sample #7 showed the strongest silicone signals in a swath roughly 600 microns wide about halfway up (tick marks 13-18).

[redacted]

Spectra from sample #7 showed another organic residue in the top shiny area, about 700 microns (0.03") high. The grey box at 3000 cm-1 contains peaks indicating C-H bonds of organic material. Low signal to noise, and broad inorganic peaks obscure more detailed interpretation of the identity.

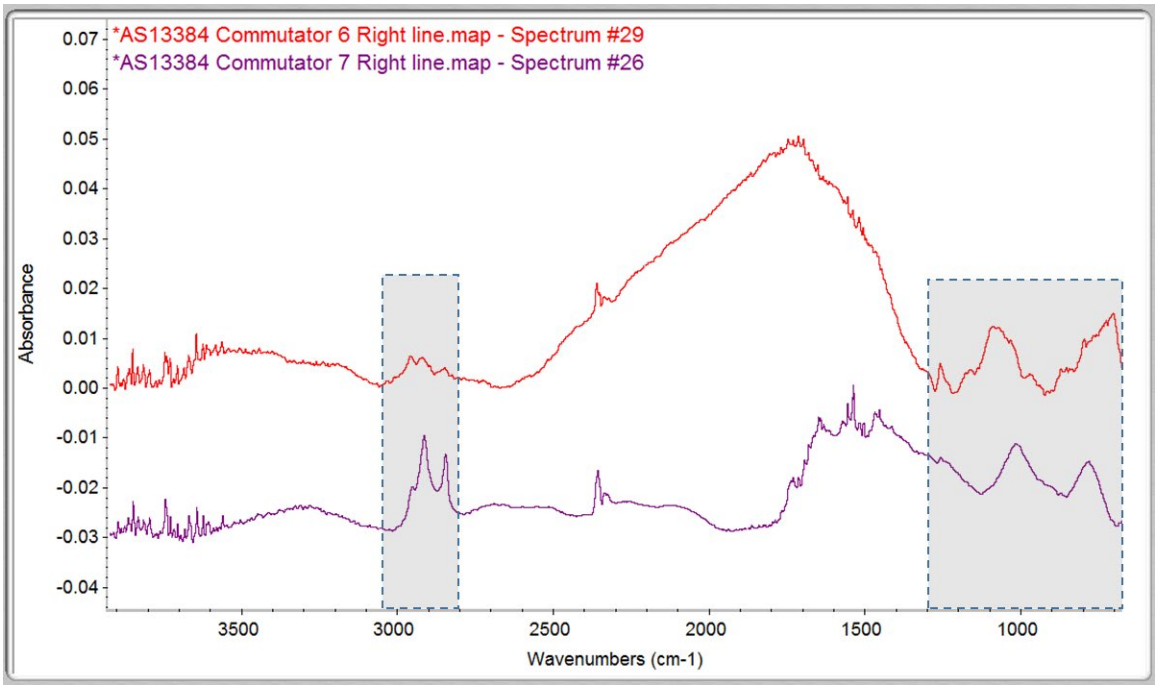

Figure 3. Unusual scans included a large inorganic peak from the dark line at the top of Sample #6, and an organic compound in the light area in the top third of #7. Both spectra also show silicone character.

Conclusions

Most of the surfaces in sample #6 and #7 were free of organic material.

Each commutator had traces of silicone. The highest concentrations of silicone were observed in locations with dark stripes, though not all dark stripes had silicone.

Sample #7 had another organic residue in addition to silicone. That was observed in the top shiny area. Low signal to noise, and broad inorganic peaks obscure more detailed interpretation of the identity of this "other" organic.

Prepared by [redacted]

October 1, 2021
Date

Acknowledgements: [redacted]

[redacted]

BOEING RESEARCH & TECHNOLOGY
Manufacturing and Manufacturing Technology
Chemical Technologies - Analytical Laboratories

Date: November 15, 2021

Analytical Chemistry Lab

[redacted]

[redacted]

DISTRIBUTION

To: [redacted]
Cc: [redacted]

Subject: AS13384-Brush Analysis - Material identification on the top of brushes from DC motor

Summary
Silicone was the most prevalent organic material identified on the top surfaces of Brushes “P” and “N”. No other organic materials were detected. Inorganic materials were occasionally observed. They will be better identified by X-Ray based elemental analysis.

Background
Two Brushes were removed from the DC motors by Equipment Quality Analysis (EQA) and delivered in glass petri dishes for analysis in support of Air Safety investigation AS13384-Brush Analysis.

Figure 1 shows one Brush sample, labeled “P”, with a red box drawn around the end surface to be analyzed. The Brush samples were small pieces of metal, curved and rectangular in shape, approximately 0.10” x 0.05” x 0.05”. The surface of interest on both on both Brushes was black with orange colored spots, and consistent parallel grooves.

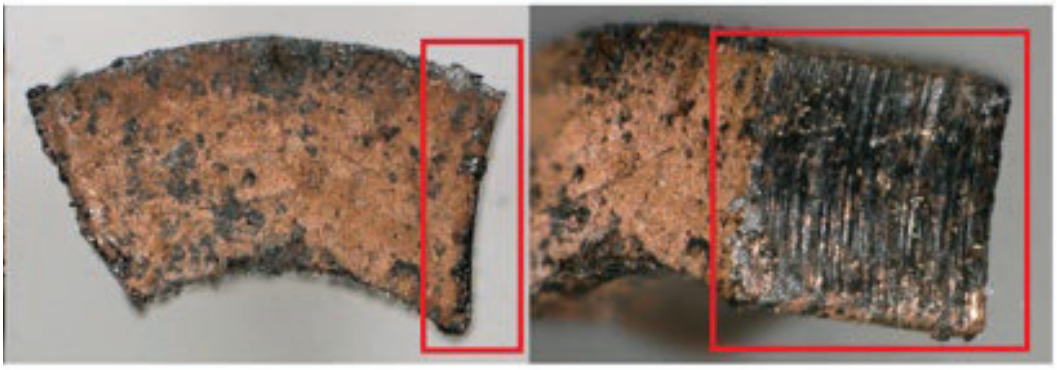

Figure 1. Brushes were small curved rectangular pieces of metal.

The request was determining any organic material present on the surfaces of interest. SEM / EDS analysis will be performed subsequently to identify inorganic materials.

Experimental

[redacted]

Samples were not cleaned or prepped beyond removing them from the vial with cleaned tweezers, and affixing them to a staging slide using double-stick tape (Figure 2). Tape positioned Brushes so the end of interest was facing up toward the instrument detector and parallel to the stage so the entire surface was in focus.

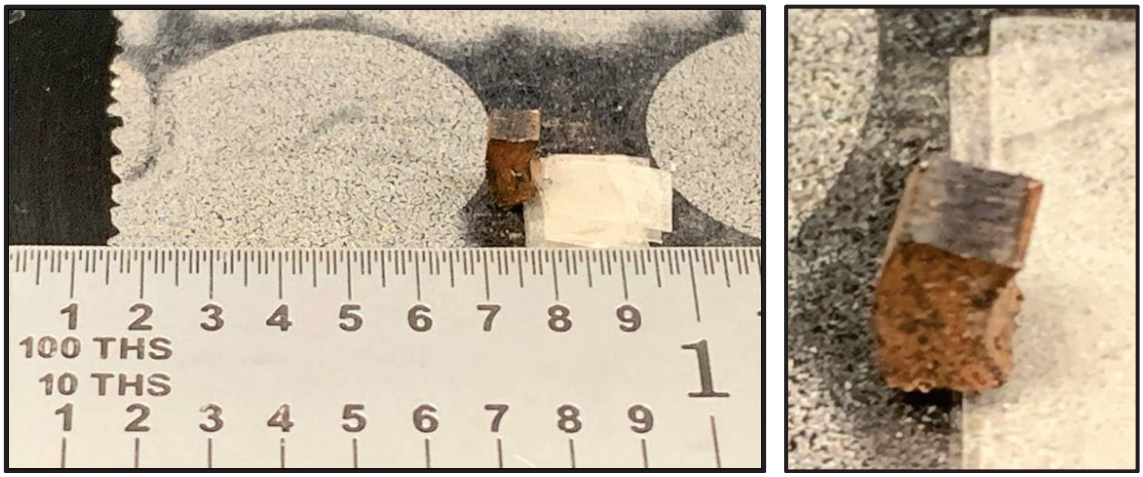

Figure 2. Pieces were positioned on the FTIR instrument stage using double-stick tape, so that the surface of interest faced up and was flat.

The sampling stage was mounted into a Thermo-Nicolet iN-10 FTIR microscope for scanning. The iN-10 was configured to generate "line maps" by collect a spectrum every 100 microns along a path set by the user, shown in Figure 3. Tick marks show where each spectrum was collected. Each sample was scanned bottom to top along the *center* line and along the *right* side.

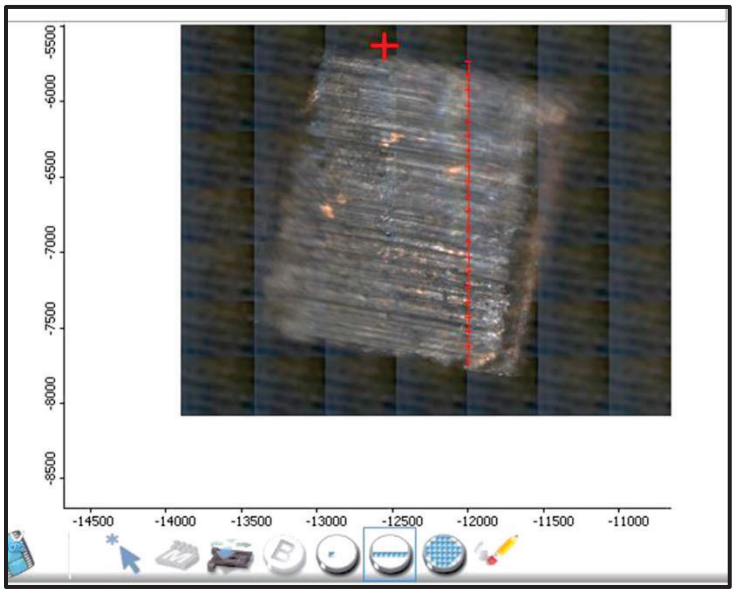

Figure 3. Red line shows where data were collected, in a "line map" along the right sides Brush N. One spectrum per tick mark, every 100 microns (0.004 inches).

[redacted]

Spectra were collected in reflectance mode, 132 scans co-averaged at 4 cm^{-1} resolution, over the range 680-4000 cm^{-1}, using a liquid nitrogen cooled MCT detector. The aperture was 100 microns x 100 microns. All spectra were screened for anomalies and trends.

Results

Surfaces of Brushes N and P showed a consistent residue of silicone. Figure 4 shows a smooth surface of higher and lower peaks of similar shape and location. Spectral features were not correlated to color of the substrate, whether black area or an orange spot.

Occasional inorganic peaks appeared in the data. Three examples were: P-center scan (600 microns and 1400 microns from the bottom), and N-right scan (900 microns from the bottom).

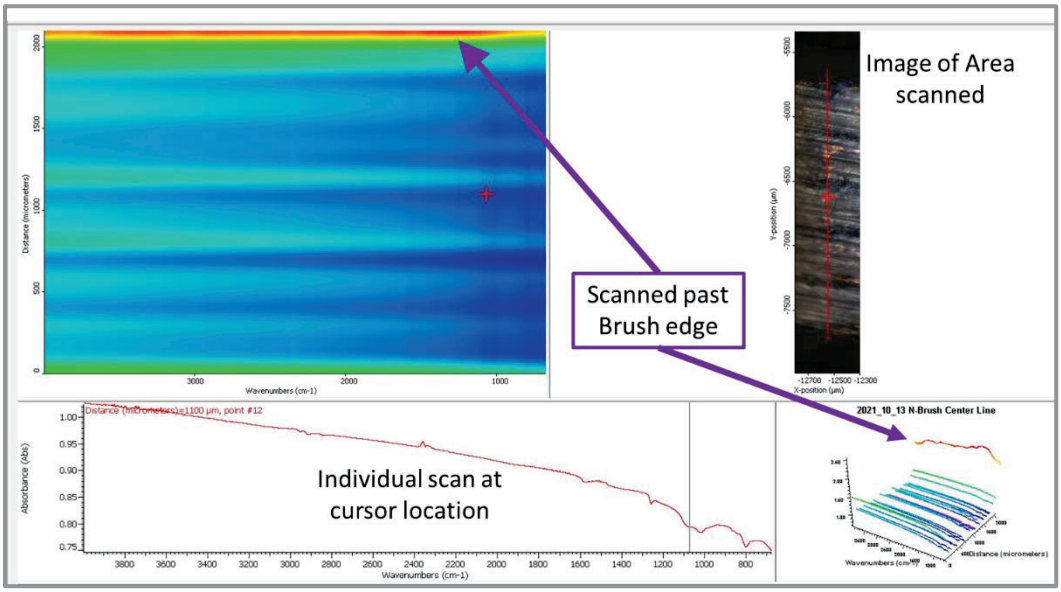

Figure 4. Smooth FTIR contour map of Brush N's center. The outlier scan noted by the arrow is where data collection went past the Brush.

Conclusions

P and N Brush surfaces had continuous layers of silicone material. Amounts of silicone varied, but in conjunction with colors of the substrate.

Occasional bits of inorganic material were detected. They may be better identified using X-Ray based electron microscopy, which detects elemental compositions.

Prepared by [redacted] November 15, 2021
Date

[redacted]

Engineering, Test & Technology
Boeing Research & Technology

AS13384 DC Motor Failure Analysis

Manufacturing Technology and Integration

December 3, 2021

Overview

For sliding electrical contact, a low and/or stable contact resistance is the most important property. Electrical contact resistance is a system property of the brush and commutators, and is as a result of the action of these surfaces in relative motion. The electrical contact resistance partly consists of a film resistance and a constriction resistance.[1]

Reliably low and stable contact resistance is the result of continuous contact of a sufficient area of copper metal on each side of the commutator/brush interface. Film resistance due to buildup of fretting debris would gradually increase the system resistance. Constriction resistance increased as available copper metal on the brush and commutator bar working surfaces decreased substantially due to wear and a difference in brush surface and bulk copper metal content. Constriction resistance is more random and prone to large spikes in resistivity due to:

- Unique surface topographies on each commutator bar.
- A changing brush topography due to differences in grinding action of each commutator bar.
- The dynamically changing availability of copper metal on the surface of the commutator bars and brush.

References

1. Grandin, M. and U. Wiklund. *"Influence of mechanical and electrical load on an copper/copper-graphite sliding electrical contact."* Tribology International 121 (2018) 1-9.

Film Resistance

- A silicone based substance is present on brush and commutator bar surface. Previous EQA analysis as well as confirmation from the motor supplier confirms the motor bearings contain silicone based lubricant and this is believed to be the source of the silicone contamination on the brush/commutator surface.

- The silicone was found to be fully dense with copper metal and Cu_2O copper oxide fretting debris, a condition that likely worsened over time and added to film resistance.

- The fretting debris was generated exclusively from the brushes. The brushes consist of softer unworked copper metal and graphite, whereas the commutator bars are made from wrought copper, further hardened at the surface by a circumferential material-removal operation. The shallow surface recrystallization from the last material-removal operation was readily apparent, indicating no fretting of the commutator surface.

- Each commutator bar would have a unique surface roughness pattern, which would accelerate the grinding action against the brushes. Burrs on the commutator bar surface were shown to act as a drag force against the brushes.

- On the commutator bars, the fretting debris-filled silicone film could potentially grow in thickness sufficient to cover the entirety of the surface at a local level. The film itself had poor contact with the commutator bar.

- On the brushes, the fretting debris-filled silicone built up mostly over the graphite and to a lesser extent the copper metal, likely increasing film resistance of each component over time.

Constriction Resistance

- The electrical contact area on the commutators was lower than the apparent work surface area, due to the initial surface roughness of the commutators.

- The as-manufactured area percent copper metal on the brush is expected to be around 48-71%. With wear, the surface enrichment of copper metal gave way to the bulk composition of 18% copper metal, increasing constriction resistance.

- An estimated 6.7% of the brush working surface was copper metal, increasing the constriction resistance beyond that expected by the bulk 18% copper metal.

- N-brush and commutator 6 were analyzed by metallography, SEM and STEM.
- Circumferential surface topography was present in the active and inactive regions, indicating it was a pre-existing condition.
- The commutator topography was imprinted on the active brush surfaces.

N-Brush

P-Brush

Commutators (resistance values obtained by valve manufacture during component examination):

1	2	3	4	5	6	7	8	9

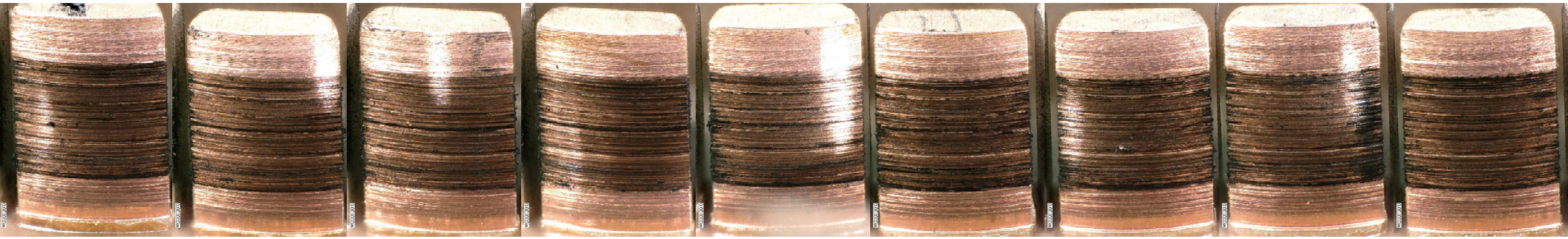

300Ω	138Ω	3200Ω	97Ω	285Ω	240,000Ω	40,000Ω	1060Ω	108Ω

- Film Resistance - A silicone based substance is present on brush and commutator bar surface. Previous EQA analysis as well as confirmation from the motor supplier confirms the motor bearings contain silicone based lubricant and this is believed to be the source of the silicone contamination on the brush/commutator surface.

FTIR Analysis Summary:

Silicone was the only organic material identified on the surfaces of commutators 6 and 7.

Overview – Specimen preparation for scanning transmission electron microscopy (STEM) by focused ion beam (FIB) in the scanning electron micrscope

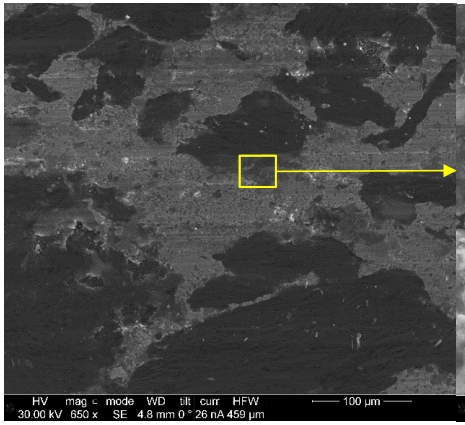

Targeting film on brush

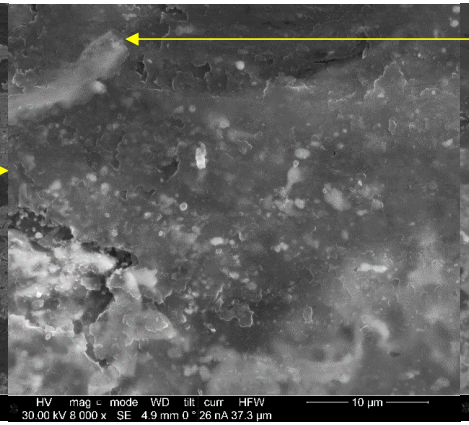

Higher magnification

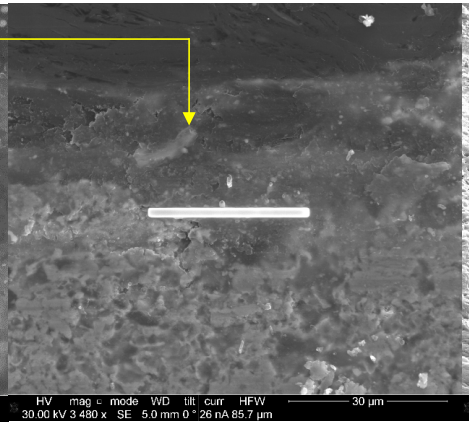

Platinum strap deposition

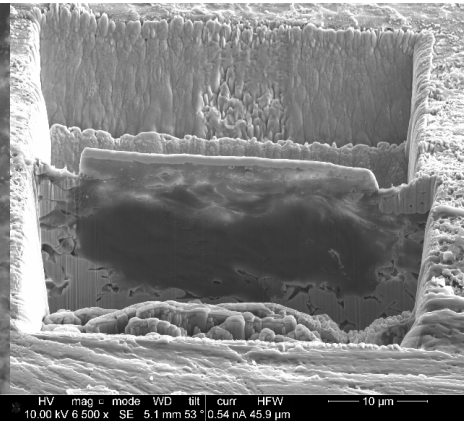

Foreground/background trough milling

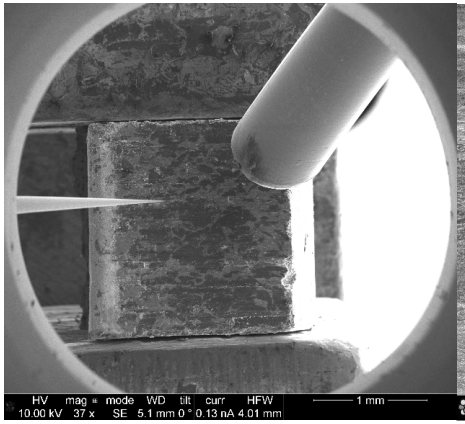

Plucker and gas insertion needles

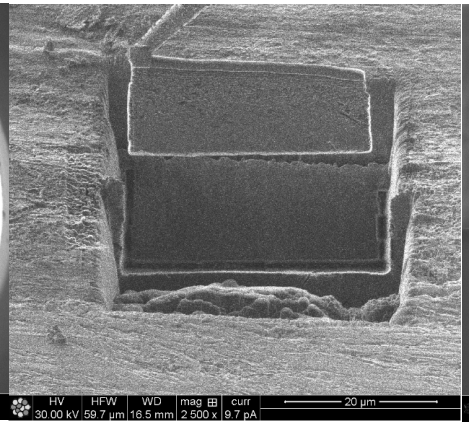

Specimen liftout

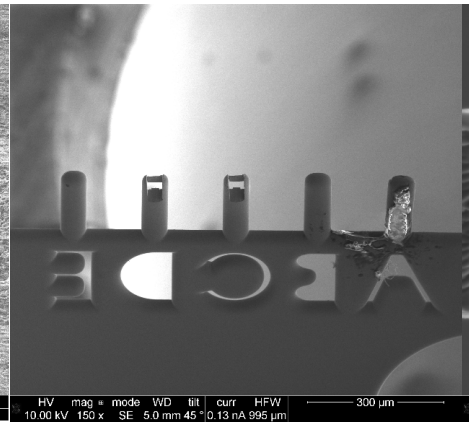

Specimens welded to grid

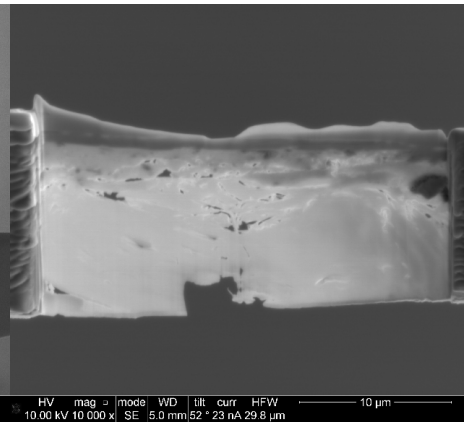

Final thinning

Film Resistance - The silicone was found to be fully dense with copper metal and Cu_2O copper oxide fretting debris, a condition that likely worsened over time and added to film resistance.

STEM-EDS map of film over brush graphite

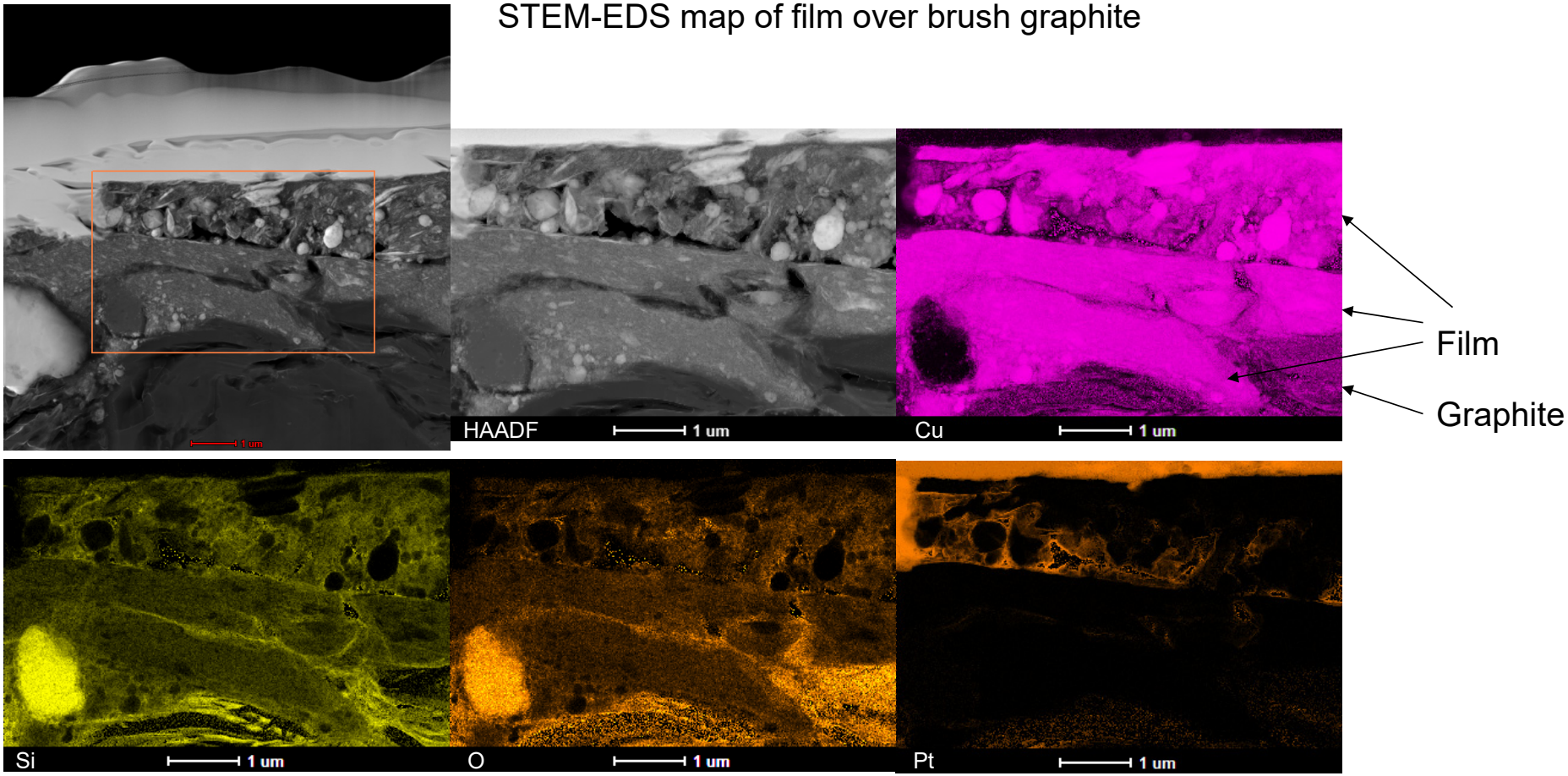

Film Resistance - The silicone was found to be fully dense with copper metal and Cu_2O copper oxide fretting debris, a condition that likely worsened over time and added to film resistance.

Brightfield STEM images of the film on the commutator bar (left) and brush (right).

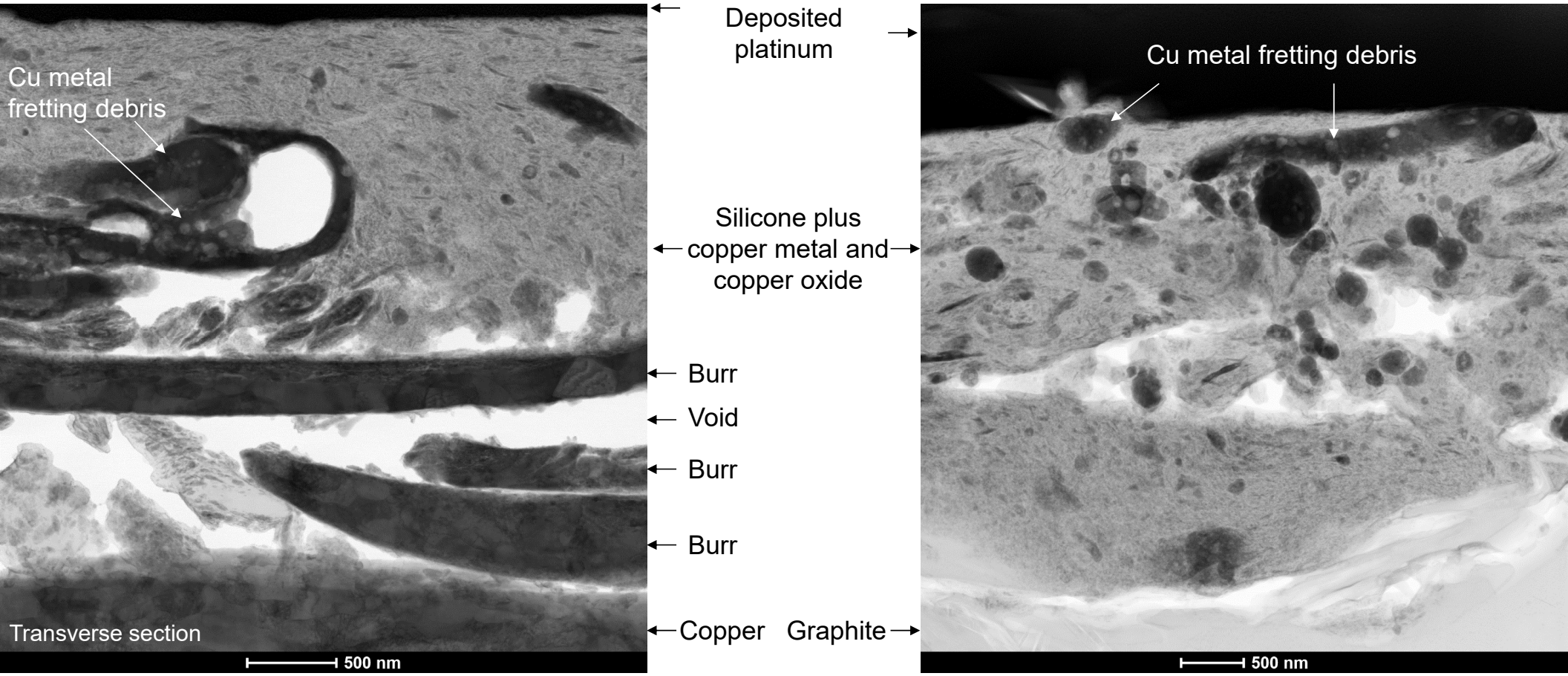

Film Resistance - The silicone was found to be fully dense with copper metal and Cu_2O copper oxide fretting debris, a condition that likely worsened over time and added to film resistance.

The primary copper component of the film was nanograined cubic Cu_2O, space group $Pn\bar{3}m$.

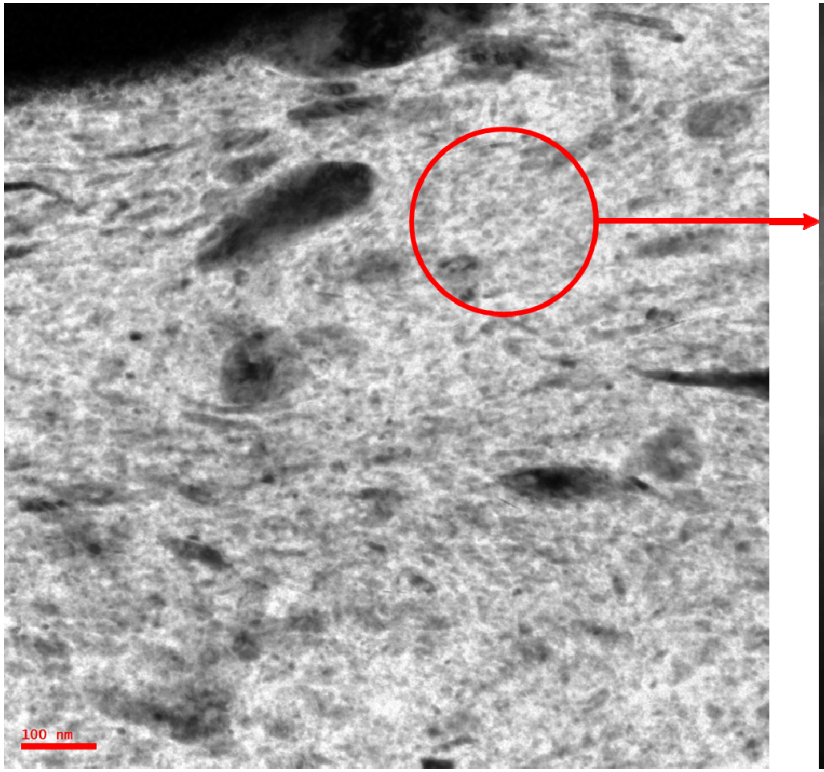

TEM image of the silicone film on the commutator, fully dense with copper oxide.

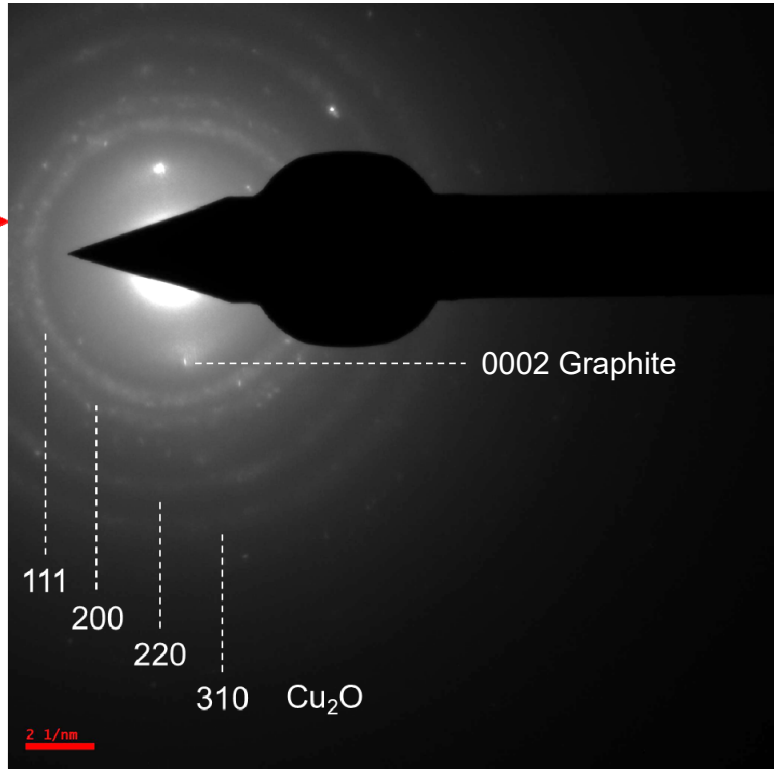

TEM electron diffraction pattern of the silicone film, exhibiting a ring pattern from nanograined Cu_2O.

Film Resistance - The fretting debris was generated exclusively from the brushes. The brushes consist of softer unworked copper metal and graphite, whereas the commutator bars are made from wrought copper, further hardened at the surface by a circumferential material-removal operation. The shallow surface recrystallization from the last material-removal operation (likely from the time of manufacture) was readily apparent, indicating no fretting of the commutator surface.

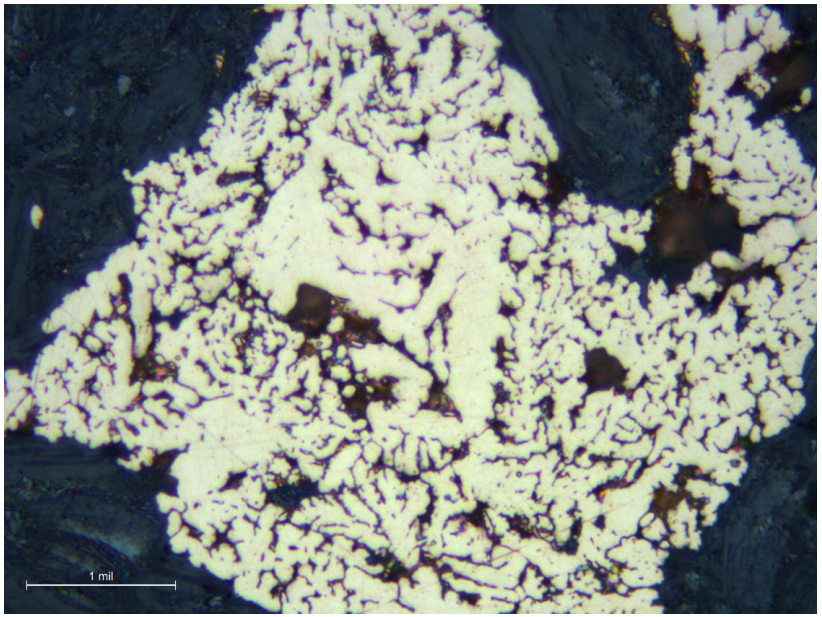

Photomicrograph showing dendritic nature of the electrolytically-deposited brush copper, which would have the hardness of cast copper.

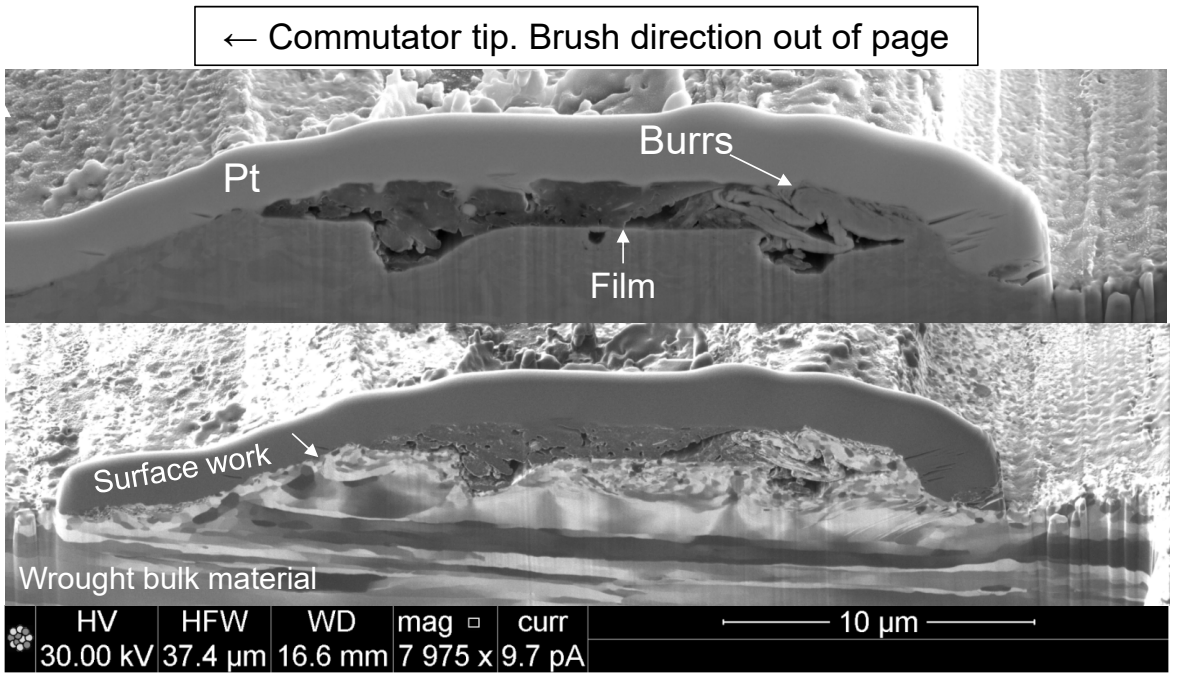

Transverse FIB section of the commutator bar with electron (top) and ion (bottom) beam imaging, showing surface work hardening and associated burrs, and wrought grains in the bulk material.

Film Resistance - Each commutator bar would have a unique surface roughness pattern, which would accelerate the grinding action against the brushes. Burrs on the commutator bar surface were shown to act as a drag force against the brushes.

SEM and STEM images of a transverse section of the commutator from within a surface topography trough that contained the silicone film.

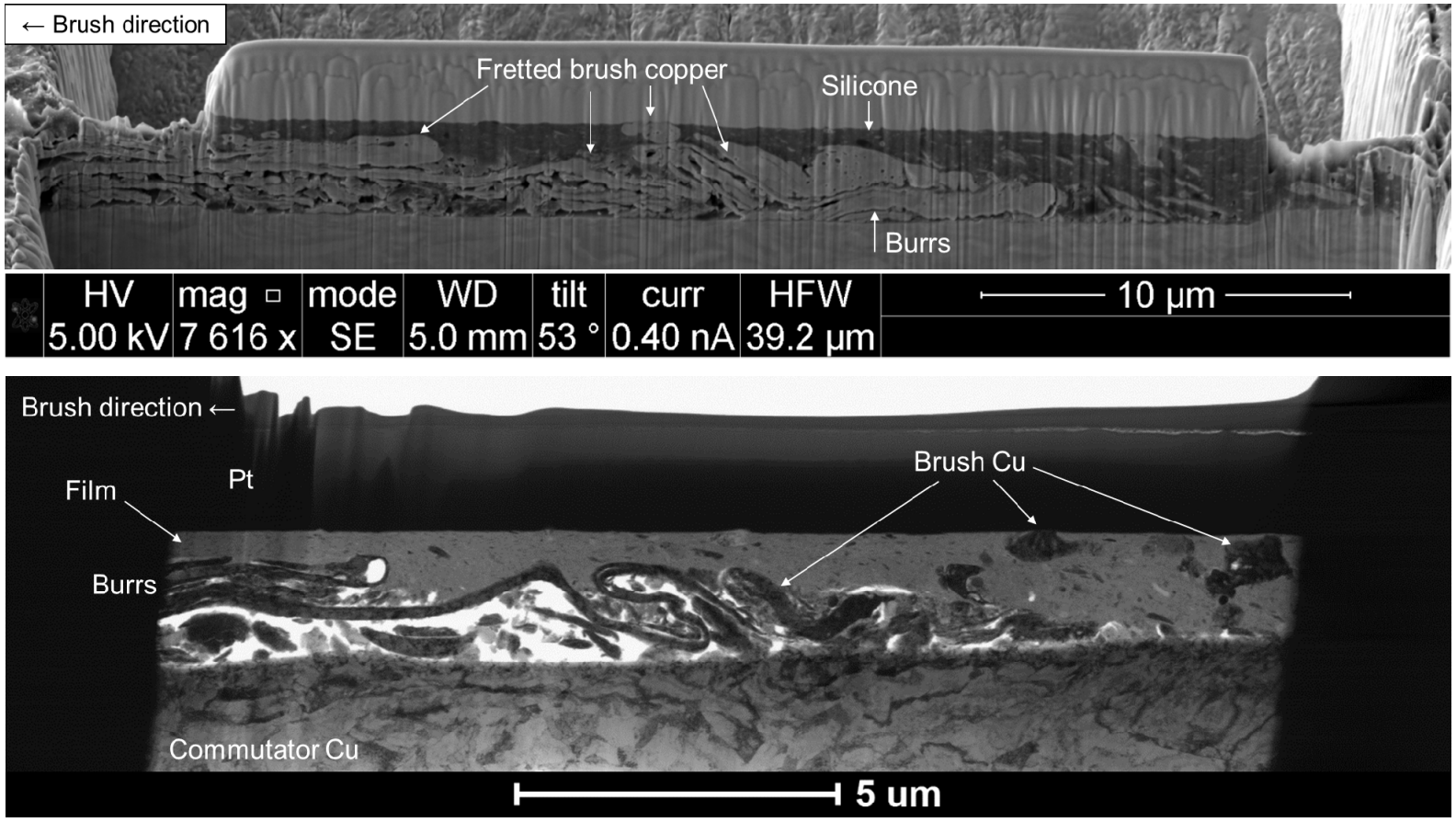

Film Resistance - On the commutator bars, the fretting debris-filled silicone film could potentially grow in thickness sufficient to cover the entirety of the surface at a local level. The film itself had poor contact with the commutator bar.

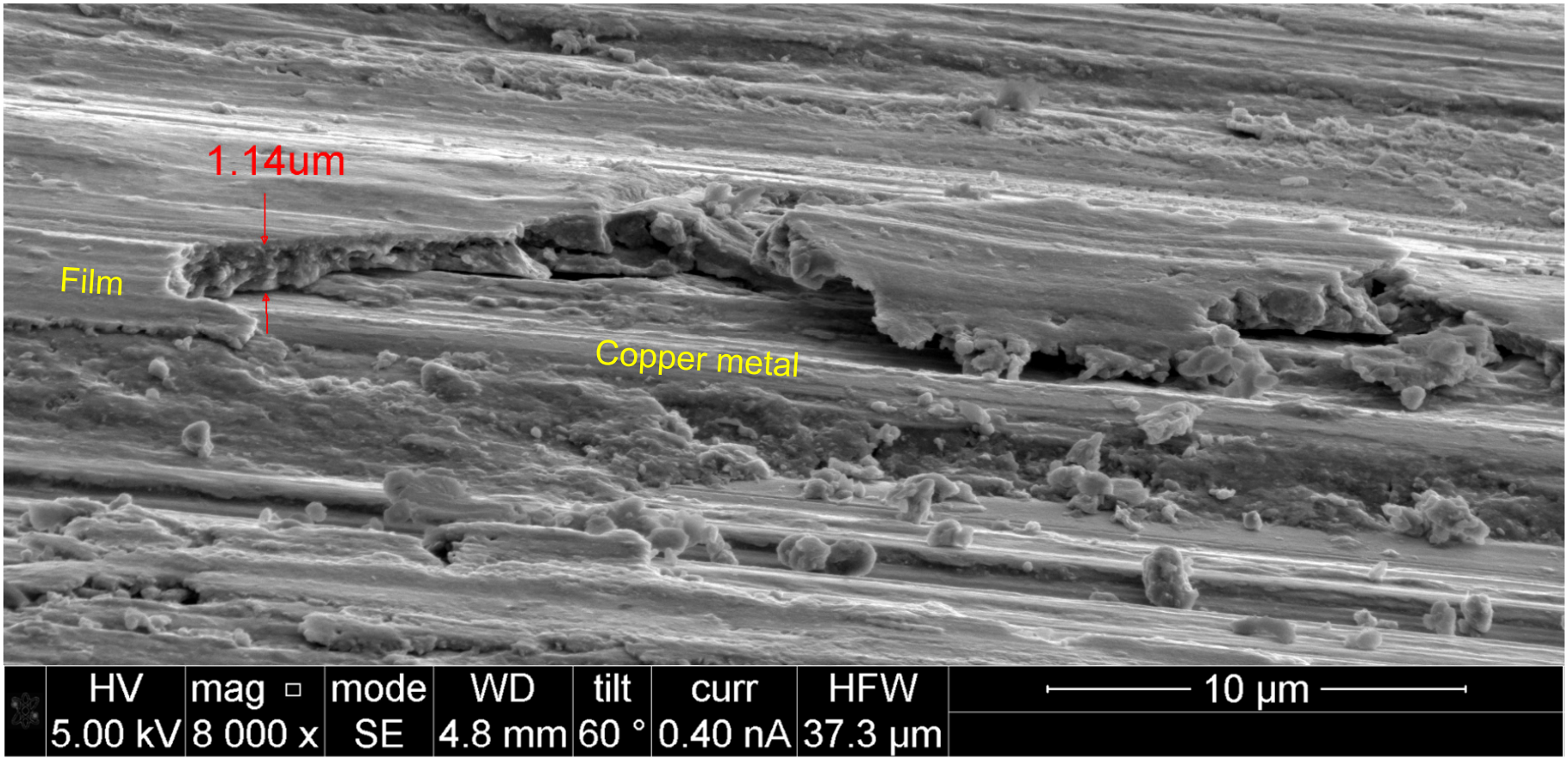

60º inclined SEM image of the commutator bar looking down the axial direction.

Film Resistance - On the brushes, the fretting debris-filled silicone built up mostly over the graphite and to a lesser extent the copper metal, likely increasing film resistance of each component over time.

Example 1 – A FIB cross-section of brush shows silicone and fretting debris over copper metal and graphite. The wear direction is vertical in the images.

Silicone plus fretting debris

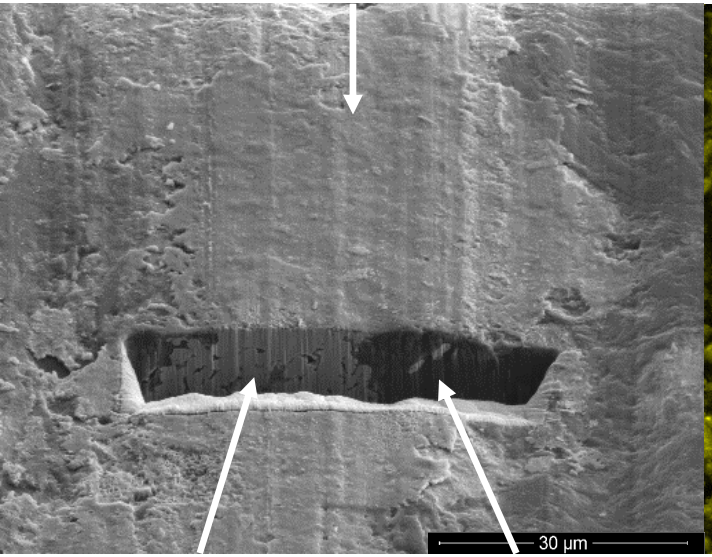

Cu metal Graphite

Silicone plus fretting debris

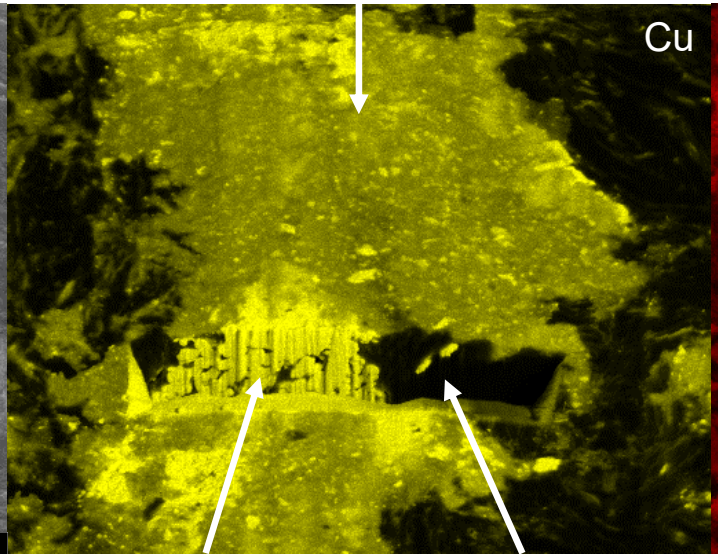

Cu metal Graphite

Silicone plus fretting debris

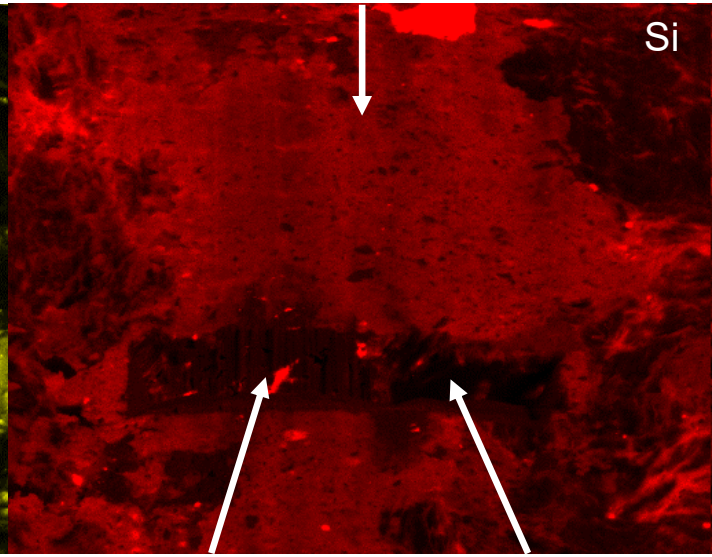

Cu metal Graphite

Film Resistance - On the brushes, the fretting debris-filled silicone built up mostly over the graphite and to a lesser extent the copper metal, likely increasing film resistance of each component over time.

Example 2 – A FIB cross-section and STEM liftout on a brush longitudinal to the wear direction shows fretting debris in silicone oil spread over graphite.

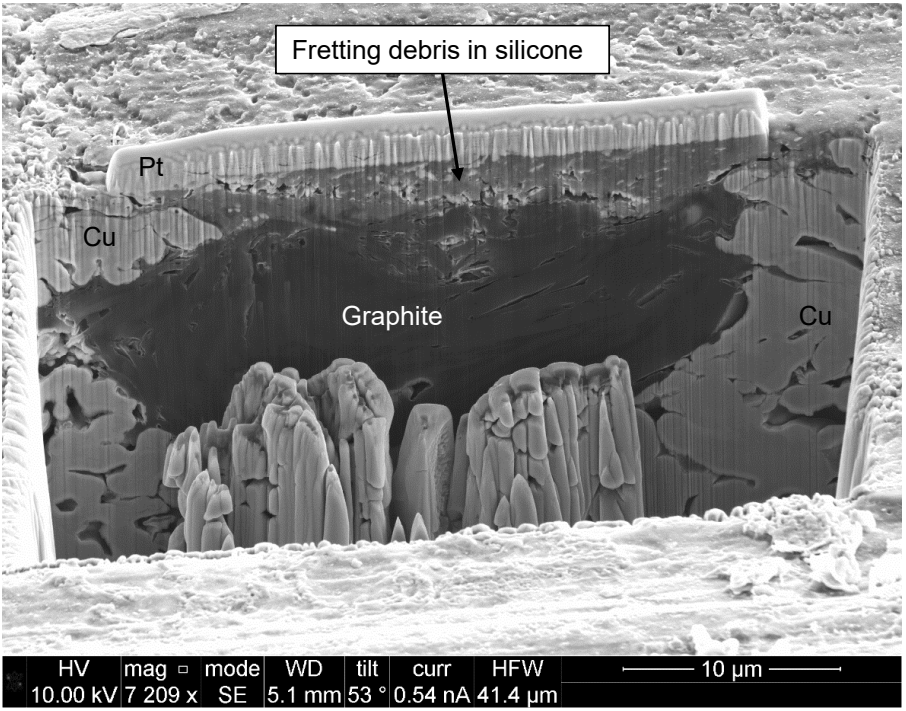

SEM

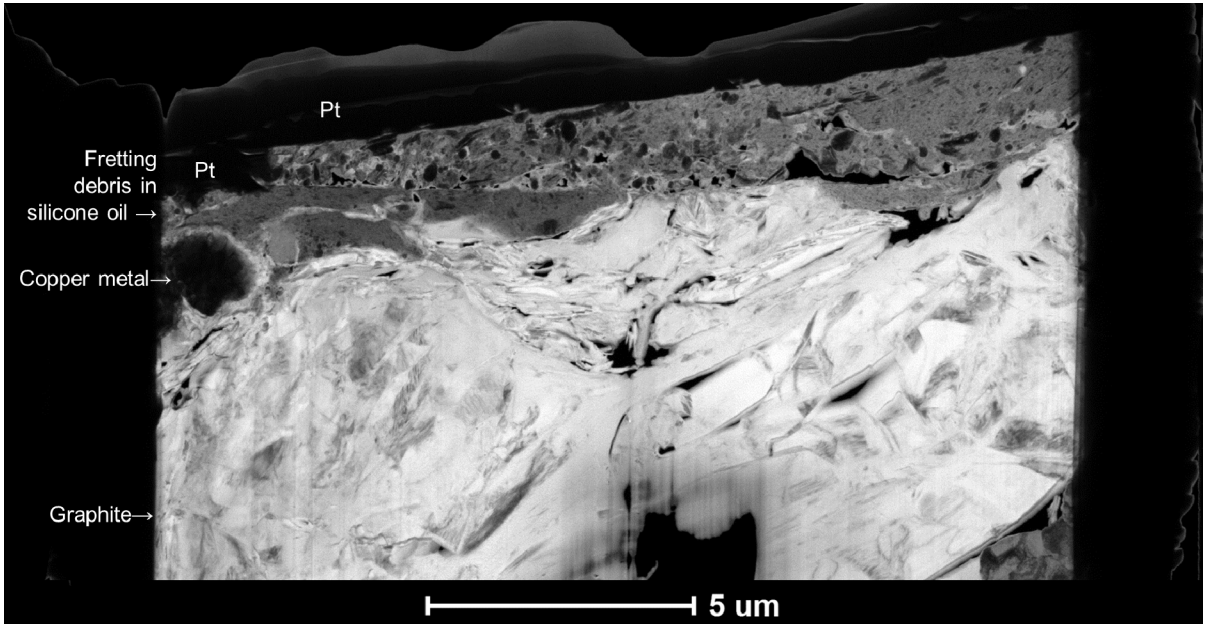

Annular darkfield STEM

Constriction Resistance - The electrical contact area on the commutators was lower than the apparent work surface area, due to the initial surface roughness of the commutators.

In the bottom of the image, there is roughly 50% constriction as the commutator surface roughness valleys retain the film during use. Higher in the image, the constriction increases as the film is retained over the high regions because surface roughness increases separation from the brush.

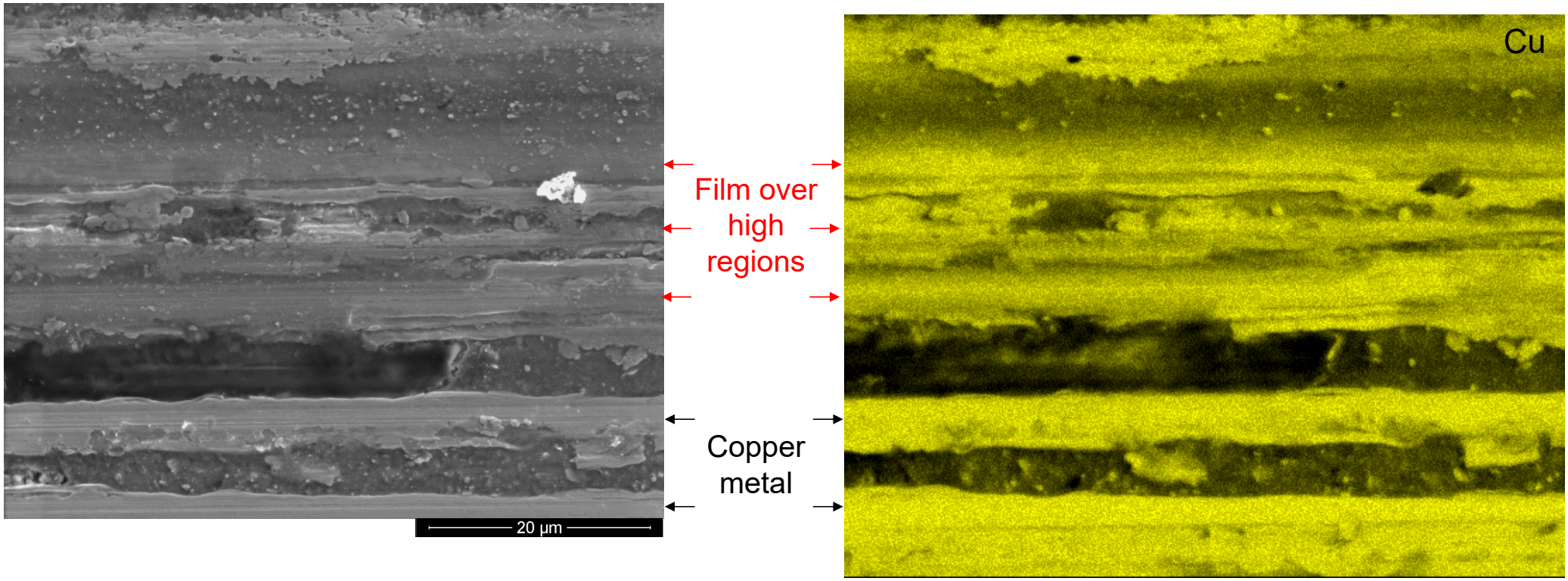

Constriction Resistance - The as-manufactured area percent copper metal on the brush is expected to be around 48-71%. With wear, the surface enrichment of copper metal gave way to the bulk composition of 18% copper metal, increasing constriction resistance.

* The working end image must be interpreted that the 50% bright area includes copper metal and silicone with fretting debris.

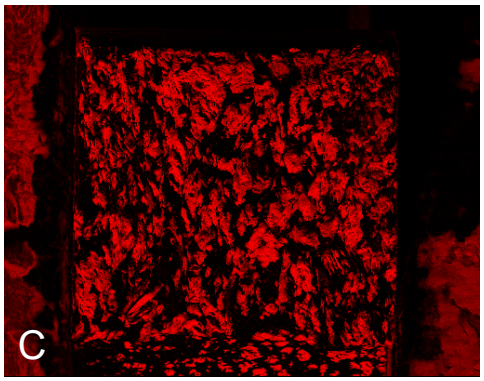

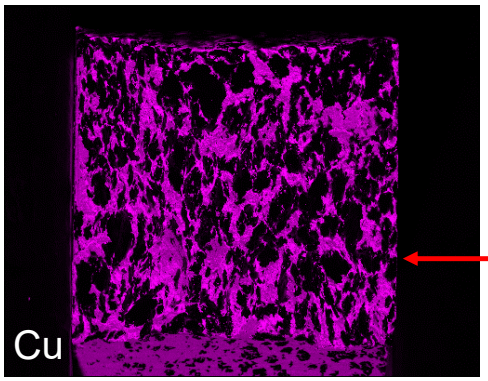

Broken end: 48% Cu / 52% graphite

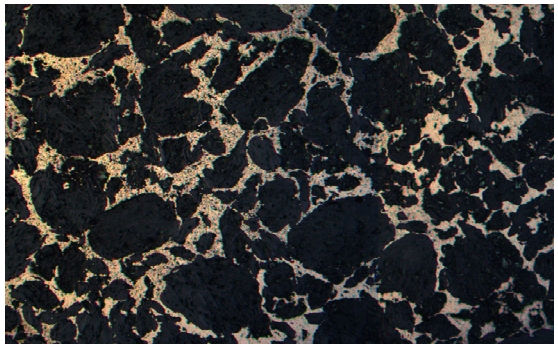

Bulk: 18% Cu / 82% graphite

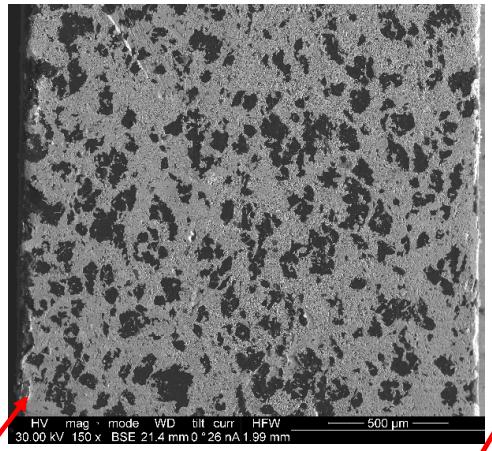

OD: 71% Cu / 29% graphite

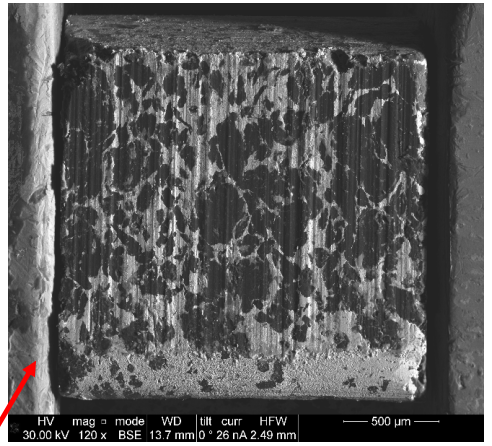

Working end: 50% Cu* / 50% graphite

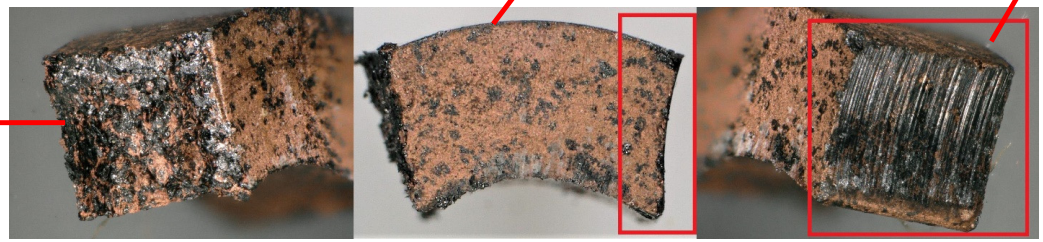

Constriction Resistance - The as-manufactured area percent copper metal on the brush is expected to be around 48-71%. With wear, the surface enrichment of copper metal gave way to the bulk composition of 18% copper metal, increasing constriction resistance.

Metallography of the brush shows surfaces can have higher copper content than the bulk composition.

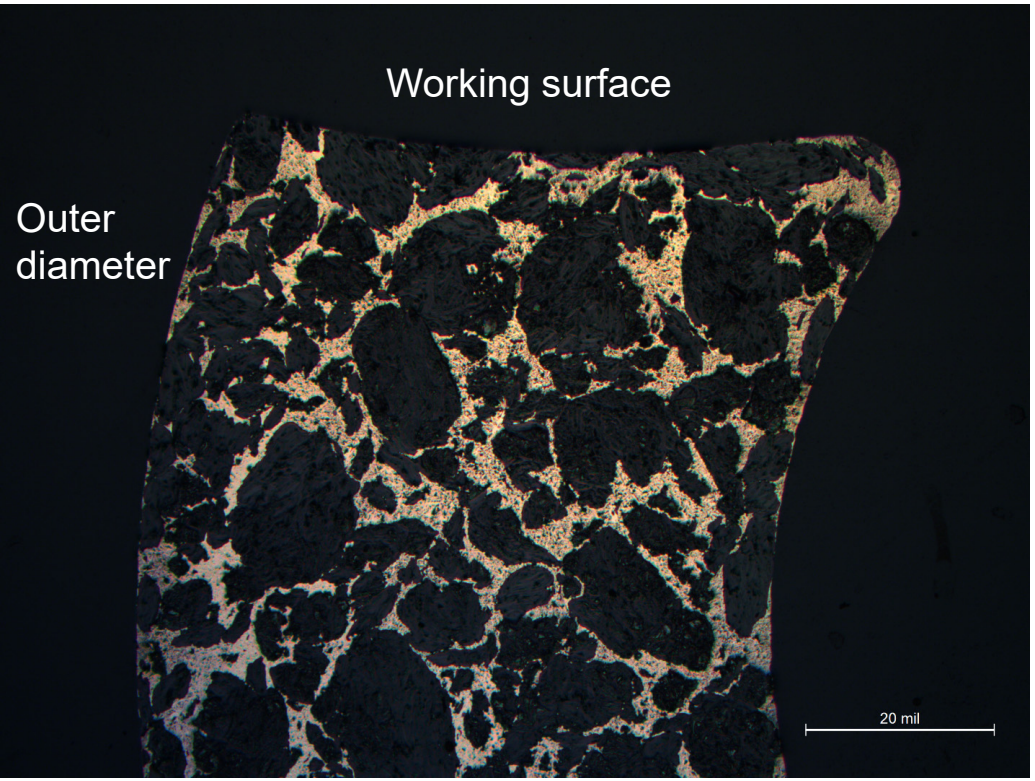

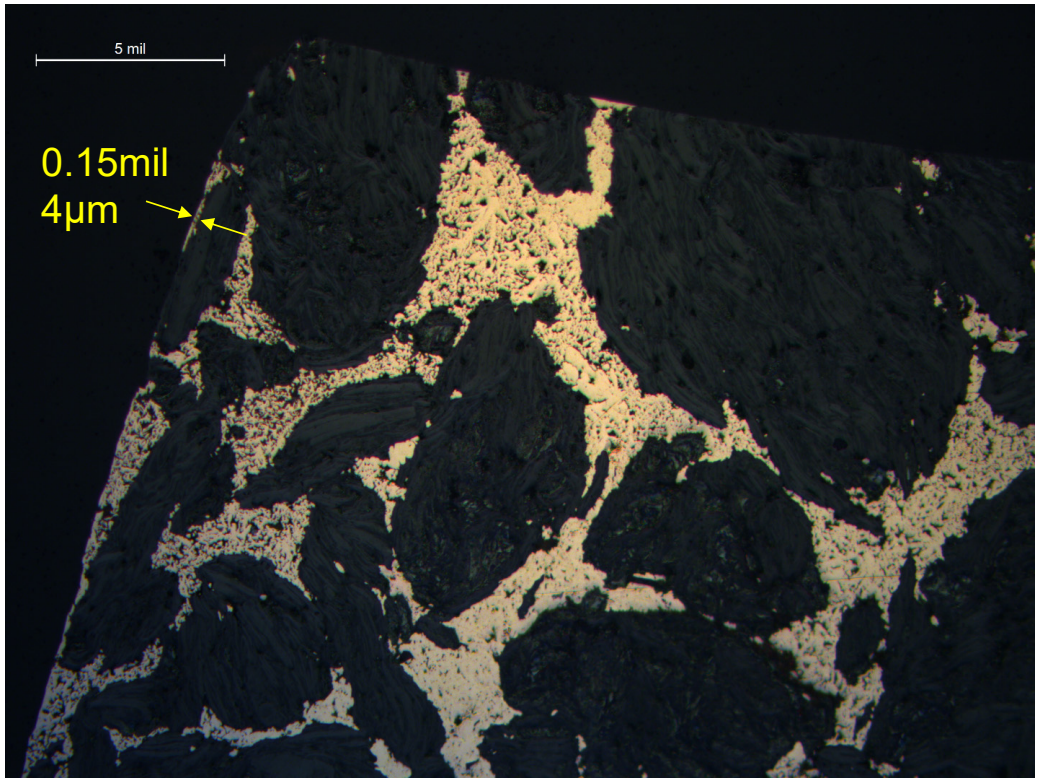

Constriction Resistance - The as-manufactured area percent copper metal on the brush is expected to be around 48-71%. With wear, the surface enrichment of copper metal gave way to the bulk composition of 18% copper metal, increasing constriction resistance.

SEM of the brush shows the working surface has less copper than the outer and inner diameter surfaces.

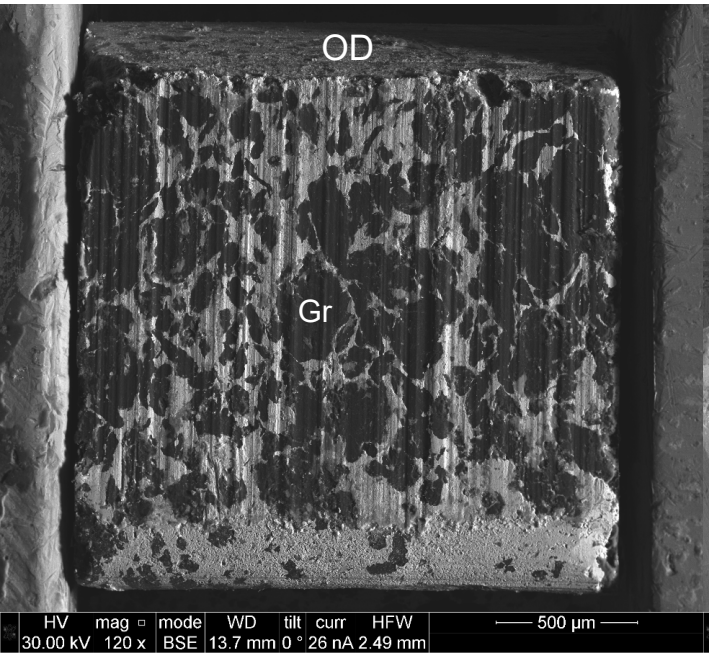

Working surface

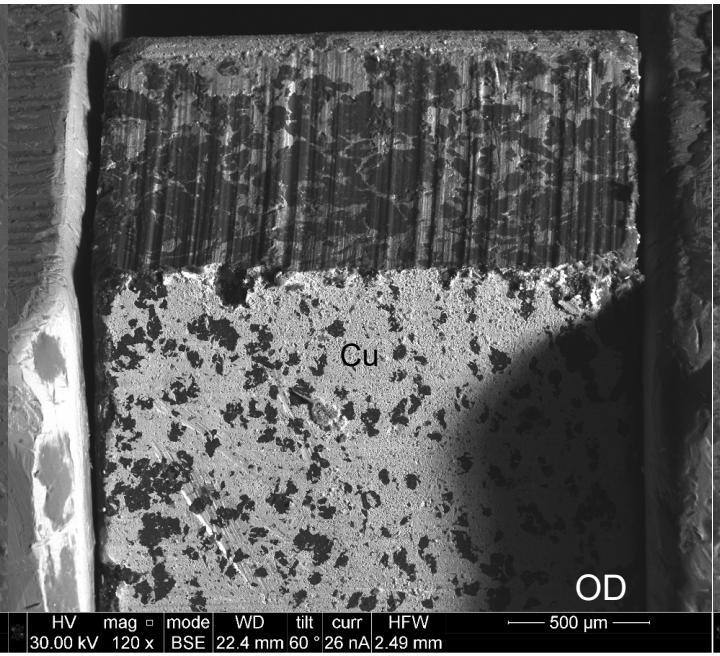

Working surface and outer diameter

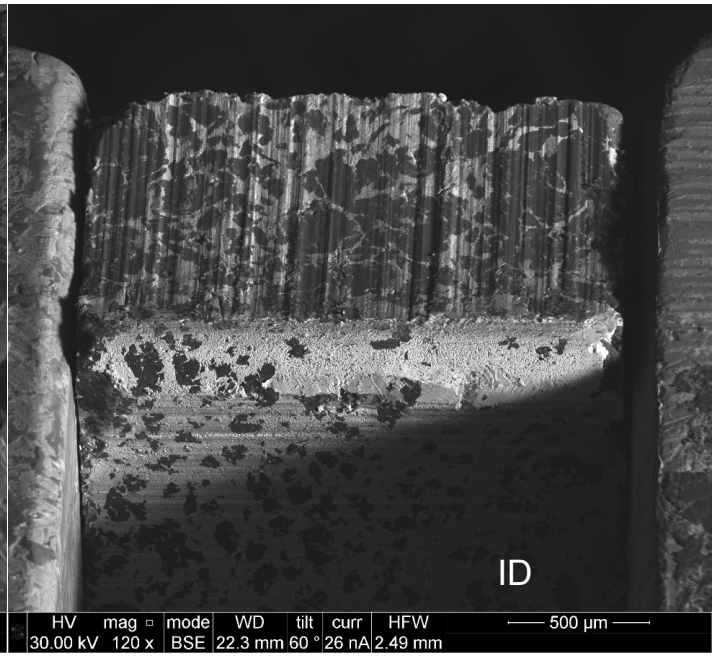

Working surface and inner diameter

Constriction Resistance - An estimated 6.7% of the brush working surface was copper metal, increasing the constriction resistance beyond that expected by the bulk 18% copper metal.

- An SEM-EDS copper map of the working surface shows brighter and darker regions, both of which are bright in the SEM image and quantified as 50% of the working surface area.
- FIB and STEM analysis have confirmed the bright regions of this map are copper metal, while the dimmer regions are Cu and Cu_2O fretting debris suspended in silicone oil.
- Image analysis of the Cu map shows 86.6% of the copper-rich areas are Cu and Cu_2O fretting debris suspended in silicone, or 43.3% of the entire working surface.
- 13.4% of the copper-rich areas are Cu metal, or 6.7% of the entire working surface.

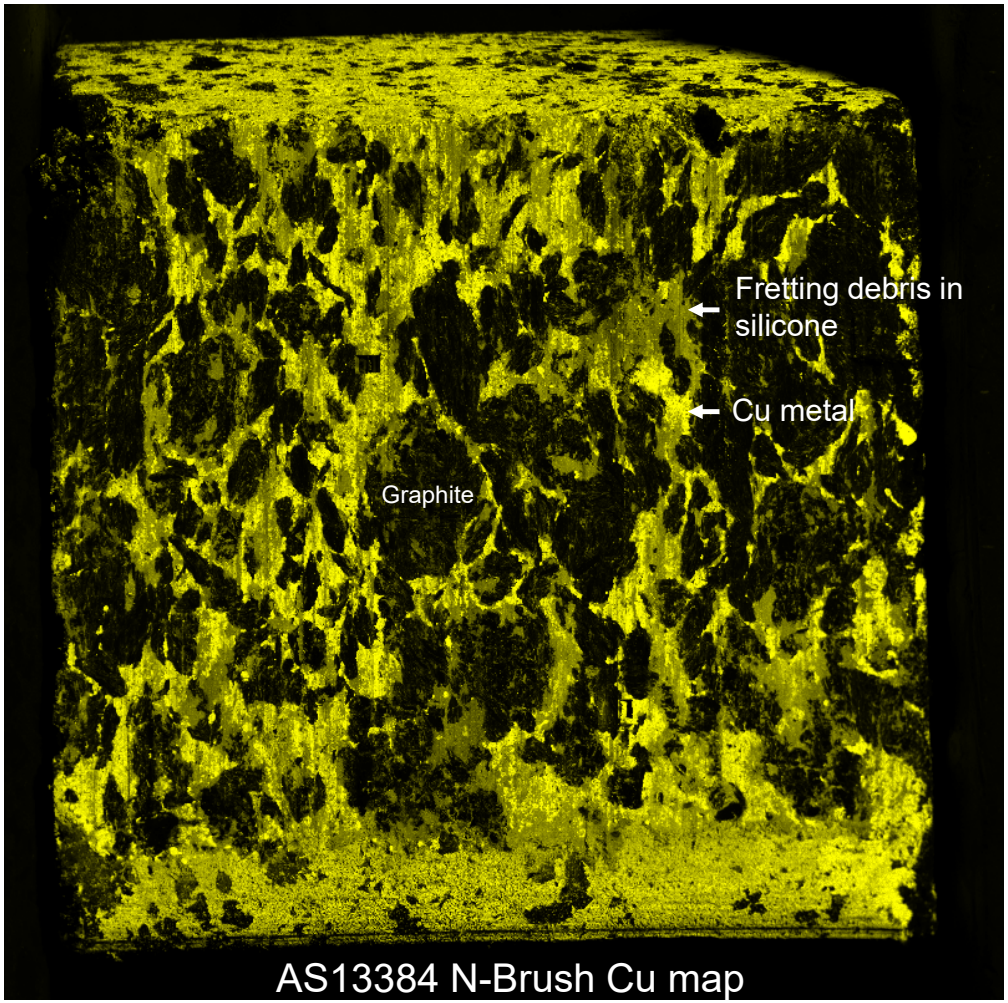

AS13384 N-Brush Cu map